Electronic Supplementary Material (ESI) for Physical Chemistry Chemical Physics.

Supplementary Information

Unraveling the electronic origin of a special feature in the triplet-minus-singlet spectra of carotenoids in natural photosystems

Agostino Migliore,[1] * Stefano Corni,[1,2] Alessandro Agostini,[1] Donatella Carbonera[1] *

[1] Department of Chemical Sciences, University of Padova, Via Marzolo 1, 35131 Padova, Italy

[2] CNR Institute of Nanoscience, 41125 Modena, Italy

* Emails: agostino.migliore@unipd.it; donatella.carbonera@unipd.it

Contents

S1. Triplet localization in the *ortho*-carotenoporphyrin dyad **S2**

S2. Properties of the electronic excitations in the model dyad **S3**

S3. Details on some electronic excitations in the model dyad **S6**

S4. Tests of computational accuracy **S9**

S5. Set of NTOs in Fig. 6 complemented with further NTOs **S10**

S6. Transition spin density for the $T_1 \rightarrow T_2$ transition in dyad's structure Q_{T_1} **S13**

S7. Shape dependence of T-S spectra on the Gaussian broadening parameter **S16**

S8. Additional NTOs and excited states for the molecular models from LHCII **S16**

S9. Properties of the singlet transitions **S31**

S10. Atomic coordinates of the M, M' and M″ systems **S34**

S1. Triplet localization in the *ortho*-carotenoporphyrin dyad

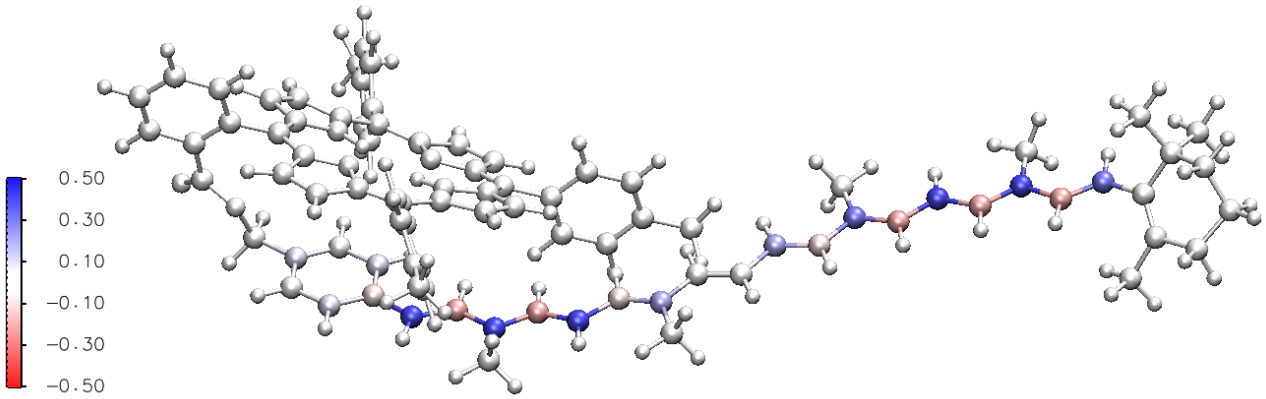

Fig. S1 Electron spin density on the *ortho*-carotenoporphyrin molecular system in tetrahydrofuran (THF) environment modeled as a polarizable continuum medium (PCM), with coordinates optimized[1] in the lowest triplet (T_1) state. We obtained the electron spin density by means of TDDFT calculation, at the ωB97X-D[2]/6-31g* level of computational accuracy, followed by Mulliken population analysis.

S2. Properties of the electronic excitations in the model dyad

This section reports the full sets of excited states obtained for the model dyad in the different PCMs, using different computational setups.

Table S1 Electronic excitations in the *ortho*-carotenoporphyrin dyad, in THF, at the indicated atomic coordinates, calculated by TDDFT at the ωB97X-D/6-31g* level of computational accuracy. Table 1 reports a subset of these transitions. The wavelengths of excitation are expressed in nm. In the notation below, $\Sigma \equiv \left\langle S^2 \right\rangle$ and n ≥ 1 (n ≥ 2) for the singlet (triplet) electronic transitions. The triplet excitations obtained with excessive spin contamination are shown in gray and not considered in the analysis.

$\lambda_{S_0 \to S_n}(Q_{S_0})$	$f_{S_0 \to S_n}(Q_{S_0})$	$\lambda_{S_0 \to S_n}(Q_{T_1})$	$f_{S_0 \to S_n}(Q_{T_1})$	$\lambda_{T_1 \to T_n}(Q_{T_1})$	$f_{T_1 \to T_n}(Q_{T_1})$	$\Sigma_{T_1 \to T_n}(Q_{T_1})$
607.94	0.0250	978.00	3.9243	2522.18	0.0000	4.229
553.25	0.0456	612.90	0.0237	967.95	0.0000	4.225
457.79	4.0941	564.48	0.0416	782.72	0.0299	2.801
403.02	0.4879	535.06	0.0097	611.02	0.0364	2.265
393.24	1.3738	517.06	0.0321	608.54	0.0003	4.192
379.98	0.8374	461.54	0.0358	603.49	0.0001	4.207
371.48	0.7042	421.88	0.1451	556.44	0.0375	2.244
342.43	0.0599	404.68	0.1140	548.51	0.0063	2.277
318.84	0.0031	388.96	1.1567	494.61	1.5593	2.268
314.64	0.0020	381.91	1.5549	484.35	2.0631	2.404
301.89	0.3048	363.28	0.1365	470.65	0.1535	2.374
291.85	0.0479	338.47	0.4172	460.41	0.6472	2.737
289.23	0.0761	319.59	0.0020	399.48	0.0207	3.275
286.47	0.1334	317.08	0.6263	395.22	1.1938	2.279
285.64	0.2092	313.90	0.0025	391.24	0.0482	4.115
280.91	0.0049	309.05	0.0259	389.24	0.7954	2.436
278.62	0.3597	301.59	0.4858	382.49	0.9468	2.310
277.71	0.0048	287.05	0.0684	382.07	0.0015	4.230
276.01	0.0255	283.10	0.0122	371.11	0.2794	2.254
274.88	0.0071	279.54	0.0127	366.11	0.0059	4.154

Table S2 Triplet excitations in dyad structure Q_{T_1} obtained from ωB97X-D/6-31g* computations in vacuum (subscript v), and in polarizable continuous media that mimic the interior of proteins (p) and the tetrahydrofuran solvent (THF).

λ_{THF}	f_{THF}	Σ_{THF}	λ_{p}	f_{p}	Σ_{p}	λ_{v}	f_{v}	Σ_{v}
2522.18	0.0000	4.229	2715.96	0.0000	4.232	2916.05	0.0000	4.234
967.95	0.0000	4.225	959.66	0.0000	4.228	948.64	0.0000	4.231
782.72	0.0299	2.801	784.34	0.0336	2.810	784.29	0.0318	2.816
611.02	0.0364	2.265	610.97	0.0279	2.282	611.66	0.0004	4.176
608.54	0.0003	4.192	610.04	0.0003	4.198	610.85	0.0134	2.639
603.49	0.0001	4.207	606.32	0.0002	4.200	609.66	0.0027	3.875
556.44	0.0375	2.244	554.30	0.0351	2.245	552.11	0.0270	2.246
548.51	0.0063	2.277	548.03	0.0039	2.282	547.26	0.0022	2.286
494.61	1.5593	2.268	486.49	1.9835	2.271	473.10	0.2761	2.352
484.35	2.0631	2.404	479.13	1.3483	2.517	472.38	1.6031	2.696
470.65	0.1535	2.374	462.34	0.0991	2.505	452.54	1.3630	2.424
460.41	0.6472	2.737	456.77	0.9869	2.503	444.69	0.9268	2.339
399.48	0.0207	3.275	400.49	0.0170	3.250	402.02	0.0320	3.049
395.22	1.1938	2.279	395.96	0.0035	4.196	401.32	0.0016	4.127
391.24	0.0482	4.115	392.88	0.3389	2.463	396.59	0.0153	2.769
389.24	0.7954	2.436	388.62	1.0407	2.270	390.01	0.0000	4.236
382.49	0.9468	2.310	386.26	0.0002	4.232	381.86	1.1303	2.242
382.07	0.0015	4.230	378.89	1.4523	2.252	368.94	1.0232	2.305
371.11	0.2794	2.254	366.95	0.0068	4.142	367.04	0.0411	4.162
366.11	0.0059	4.154	364.46	0.2488	2.313	359.07	0.3464	2.389

Table S3 Triplet excitations in the Q_{S_0} structure of the *ortho*-carotenoporphyrin dyad in THF.

λ_{THF}	f_{THF}	Σ_{THF}
3550.25	0.0001	2.099
1505.84	0.0000	4.129
1332.44	0.0003	2.165
764.31	0.0003	4.017
694.63	0.0423	2.337
658.79	0.1249	2.147
621.25	0.0515	2.900
543.79	0.0091	3.884
518.02	0.0903	2.477
484.54	0.0148	2.575
481.77	0.0152	2.534
457.74	0.2095	2.366
454.73	3.8475	2.167
439.30	0.0995	2.355
424.09	0.1634	2.522
418.76	0.1033	3.504
417.66	0.0245	2.417
413.36	0.4618	2.471
412.30	0.0142	2.172
407.34	0.1000	2.336

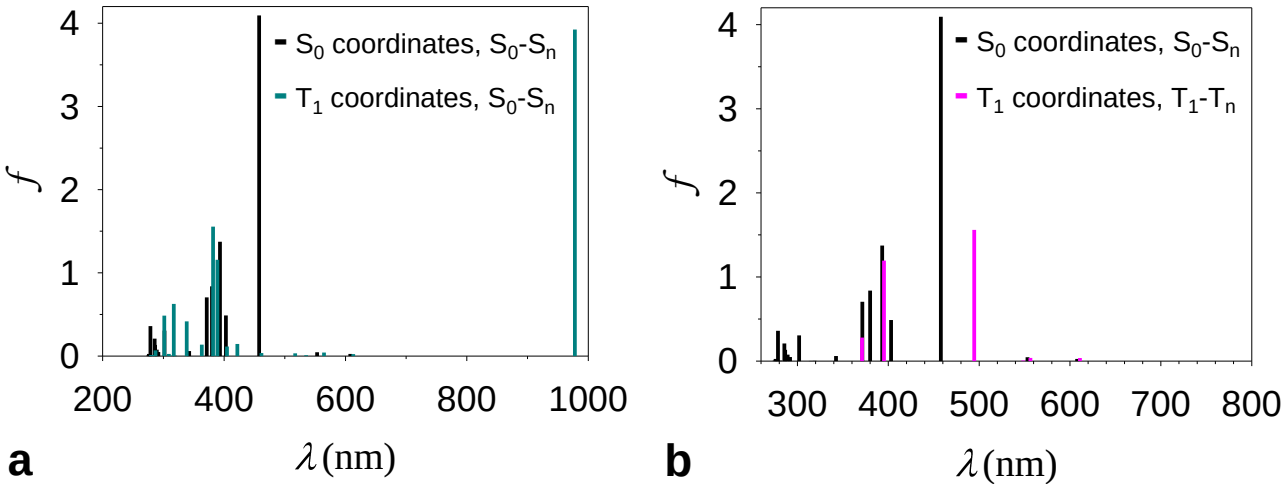

Fig. S2 (a) and (b) show the electronic transitions as in Figs. 4a and 4c, respectively, over wider spectral ranges.

Table S4 Triplet excitations in dyad structure Q_{S_0} in protein-interior medium (p) and in vacuum (v).

λ_p	f_p	Σ_p	λ_v	f_v	Σ_v
3427.04	0.0002	2.102	3310.03	0.0001	2.103
1549.24	0.0000	4.132	1574.18	0.0000	4.133
1360.12	0.0003	2.164	1387.44	0.0002	2.163
770.43	0.0001	4.057	773.55	0.0001	4.080
686.13	0.0502	2.316	674.72	0.0515	2.321
655.60	0.0949	2.150	648.04	0.0538	2.160
626.41	0.0471	2.870	628.80	0.0323	2.827
547.77	0.0113	3.762	552.86	0.0176	3.252
526.04	0.0597	2.604	535.63	0.0228	3.116
489.28	0.0077	2.507	492.94	0.0031	2.415
484.10	0.0163	2.625	486.90	0.0129	2.725
459.76	0.0030	2.395	460.43	0.0002	2.406
449.45	4.0035	2.152	444.35	0.0297	2.382
440.34	0.1031	2.372	435.26	3.7246	2.160
422.76	0.0514	3.233	425.67	0.0643	2.216
421.66	0.0048	2.745	422.71	0.0026	4.031
420.24	0.0560	2.336	420.30	0.0671	2.304
416.13	0.1104	2.491	417.99	0.0047	2.201
414.23	0.0422	2.204	409.06	0.1661	2.287
407.78	0.5509	2.415	400.19	0.5355	2.457

S3. Details on some electronic excitations in the model dyad

In this section we report some details on relevant electronic excitations in the molecular dyad derived from the output files of the Gaussian 16 program.[3]

$\mathbf{S_0}(Q_{T_1}) \rightarrow \mathbf{S_n}(Q_{T_1})$ transition in THF (central panel in Table S1)

$\mathbf{S_0} \rightarrow \mathbf{S_1}$: excitation energy = 1.2677 eV, wavelength = 978.00 nm, f = 3.9243

main single-particle transition involved and corresponding coefficient:

321 → 322 0.69446

Molecular Orbital (MO) 321 = HOMO, MO 322 = LUMO. The largest electron density of the HOMO is on a C atom of the carotenoid moiety, which is C8' using the nomenclature of ref. 1. The highest density of the LUMO is on C4 of carotenoid. This excited state is not found for the S_0 structure.

A similar description of the transition is obtained using the 6-31g** (excitation energy = 1.2652 eV, wavelength = 979.96 nm, f = 3.9159) and cc-pVDZ (excitation energy = 1.2421 eV, wavelength = 998.16 nm, f = 3.9101) basis sets, as well as other exchange-correlation functionals such as M06-2X (excitation energy = 1.3083 eV, wavelength = 947.69 nm, f = 3.8576) and M11 (excitation energy = 1.3083 eV, wavelength = 947.66 nm, f = 3.8499).

$\mathbf{S_0 \rightarrow S_2}$: excitation energy = 2.0229 eV, wavelength = 612.90 nm, f = 0.0237

main single-particle transitions involved and corresponding coefficients:

318 → 323	0.14669	
318 → 324	0.16373	
319 → 323	-0.29132	HOMO – 2 → LUMO + 1
319 → 324	-0.21832	
320 → 323	-0.35168	HOMO – 1 → LUMO + 1
320 → 324	0.41448	HOMO – 1 → LUMO + 2
321 → 324	-0.13903	

MO 319 and MO 320, which are the HOMO – 2 and HOMO – 1, respectively, are well localized on the tetrapyrrole. The same holds for MO 323 (LUMO + 1) and MO 324 (LUMO + 2), which are essentially degenerate.

Therefore, the transition mainly takes place in the porphyrin part, with a secondary contribution of a (single-particle) excitation from the carotenoid component of the dyad, as the maximum electron density of MO 321 is on atom C8' of the carotenoid component.

This electronic excitation is similar to the one at 607.94 nm that occurs in the S_0 structure (see below).

$\mathbf{S_0}(Q_{S_0}) \rightarrow \mathbf{S_1}(Q_{S_0})$ transition in THF (left panel in Table S1)

excitation energy = 2.0394 eV; wavelength = 607.94 nm; f = 0.0250

main single-particle transitions involved and corresponding coefficients:

318 → 323	-0.13928	
319 → 322	0.21739	
319 → 323	-0.33477	HOMO – 2 → LUMO + 1
320 → 322	0.48034	HOMO – 1 → LUMO
320 → 323	0.26896	HOMO – 1 → LUMO + 1
321 → 323	-0.11306	

The HOMO – 1 is localized on the tetrapyrrole and is very similar to the corresponding MO in the Q_{T_1} structure. The HOMO – 2 also is localized on the tetrapyrrole.

LUMO and LUMO + 1 are very similar in energy and spatial distribution to the LUMO + 1 and LUMO + 2, respectively in the Q_{T_1} nuclear conformation.

$T_1(Q_{T_1}) \rightarrow T_2(Q_{T_1})$ transition in THF (right panel in Table S1)

excitation energy = 2.0291 eV; wavelength = 611.02 nm; f = 0.0364; $\langle S^2 \rangle = 2.265$

main single-particle transitions involved and corresponding coefficients:

319A → 323A	-0.30575	αHOMO – 3 → αLUMO
319A → 324A	-0.33330	αHOMO – 3 → αLUMO + 1
320A → 323A	-0.29855	
320A → 324A	0.40475	αHOMO – 2 → αLUMO + 1
321A → 324A	-0.19194	
318B → 322B	0.14552	
319B → 322B	-0.37604	
320B → 321B	-0.16241	
320B → 322B	-0.15876	
320B → 323B	0.52343	βHOMO → βLUMO + 3

The αHOMO – 2 is localized on the tetrapyrrole. This MO is similar to the HOMO – 1 of the Q_{T_1} structure in the singlet spin state, which is involved in the $S_0(Q_{T_1}) \rightarrow S_2(Q_{T_1})$. The αHOMO – 3 also has the highest density on the tetrapyrrole. Similar considerations hold for the αLUMO and αLUMO + 1, which are essentially degenerate and very similar to the LUMO + 1 and LUMO + 2 of the same Q_{T_1} structure in the singlet spin state. Regarding the βMOs, we just mention that βMO 320 resembles the corresponding spin-up MO.

S4. Tests of computational accuracy

Table S5 reports the properties of the triplet excitations in the Q_{T_1} structure of the molecular dyad in THF environment, obtained by TDDFT computations with the ωB97X-D functional and the indicated basis sets. The electronic excitations are similarly identified using the different computational setups, although the acceptability of their spin contamination can depend on the basis set, thus showing that the chosen threshold for the spin contamination is arbitrary to some relatively small extent.

Table S5 Basis set effects

$\lambda_{T_1\rightarrow T_n}^{6-31g^*}$	$f_{T_1\rightarrow T_n}^{6-31g^*}$	$\Sigma_{T_1\rightarrow T_n}^{6-31g^*}$	$\lambda_{T_1\rightarrow T_n}^{6-31g^{**}}$	$f_{T_1\rightarrow T_n}^{6-31g^{**}}$	$\Sigma_{T_1\rightarrow T_n}^{6-31g^{**}}$	$\lambda_{T_1\rightarrow T_n}^{cc\text{-}pVDZ}$	$f_{T_1\rightarrow T_n}^{cc\text{-}pVDZ}$	$\Sigma_{T_1\rightarrow T_n}^{cc\text{-}pVDZ}$
2522.18	0.0000	4.229	2513.60	0.0000	4.229	2431.70	0.0000	4.218
967.95	0.0000	4.225	968.07	0.0000	4.225	980.96	0.0000	4.214
782.72	0.0299	2.801	783.72	0.0287	2.801	782.06	0.0313	2.766
611.02	0.0364	2.265	611.40	0.0363	2.265	616.31	0.0355	2.236
608.54	0.0003	4.192	609.02	0.0003	4.192	611.12	0.0001	4.198
603.49	0.0001	4.207	603.70	0.0001	4.208	605.66	0.0000	4.198
556.44	0.0375	2.244	556.68	0.0364	2.244	562.34	0.0338	2.234
548.51	0.0063	2.277	549.26	0.0062	2.277	554.10	0.0081	2.265
494.61	1.5593	2.268	494.69	1.7405	2.265	499.97	2.3836	2.247
484.35	2.0631	2.404	484.60	1.8993	2.410	488.47	1.4678	2.375
470.65	0.1535	2.374	470.60	0.1272	2.376	473.79	0.1523	2.348
460.41	0.6472	2.737	461.06	0.6498	2.731	463.46	0.4098	2.780
399.48	0.0207	3.275	400.10	0.0196	3.279	401.23	0.1154	3.021
395.22	1.1938	2.279	395.68	1.1943	2.275	399.38	1.1073	2.406
391.24	0.0482	4.115	391.30	0.0845	4.022	394.30	0.5959	2.449
389.24	0.7954	2.436	389.77	0.7427	2.528	390.78	0.0323	4.164
382.49	0.9468	2.310	382.97	0.9546	2.308	386.90	1.0825	2.289
382.07	0.0015	4.230	382.17	0.0007	4.230	381.30	0.0004	4.220
371.11	0.2794	2.254	371.79	0.2864	2.251	376.06	0.3463	2.216
366.11	0.0059	4.154	366.40	0.0053	4.159	366.31	0.0019	4.182

Table S6 compares the triplet excitations obtained with the ωB97X-D and CAM-B3LYP[4] functionals. CAM-B3LYP, compared to ωB97X-D, produces more excited states affected by spin contamination.

Table S6 Triplet electronic excitations obtained with the indicated exchange-correlation functionals.

$\lambda_{\omega B97X-D}$	$f_{\omega B97X-D}$	$\Sigma_{\omega B97X-D}$	$\lambda_{CAM-B3LYP}$	$f_{CAM-B3LYP}$	$\Sigma_{CAM-B3LYP}$
2522.18	0.0000	4.229	2345.46	0.0000	4.247
967.95	0.0000	4.225	928.66	0.0000	4.242
782.72	0.0299	2.801	796.31	0.0276	2.849
611.02	0.0364	2.265	615.31	0.0002	4.221
608.54	0.0003	4.192	608.83	0.0002	4.215
603.49	0.0001	4.207	595.83	0.0410	2.259
556.44	0.0375	2.244	553.15	0.0112	2.320
548.51	0.0063	2.277	543.94	0.0288	2.285
494.61	1.5593	2.268	528.99	0.0875	2.317
484.35	2.0631	2.404	521.66	0.0805	2.332
470.65	0.1535	2.374	487.25	3.5567	2.376
460.41	0.6472	2.737	465.42	0.5904	2.833
399.48	0.0207	3.275	415.78	0.0400	2.414
395.22	1.1938	2.279	404.56	0.0325	3.345
391.24	0.0482	4.115	400.01	0.0017	4.244
389.24	0.7954	2.436	397.25	1.1697	2.273
382.49	0.9468	2.310	391.09	0.0040	4.239
382.07	0.0015	4.230	389.50	1.2372	2.305
371.11	0.2794	2.254	382.98	0.2236	2.586
366.11	0.0059	4.154	379.39	0.1710	2.751

S5. Set of NTOs in Fig. 6 complemented with further NTOs

$$S_0(Q_{S_0}) \rightarrow S_1(Q_{S_0})$$

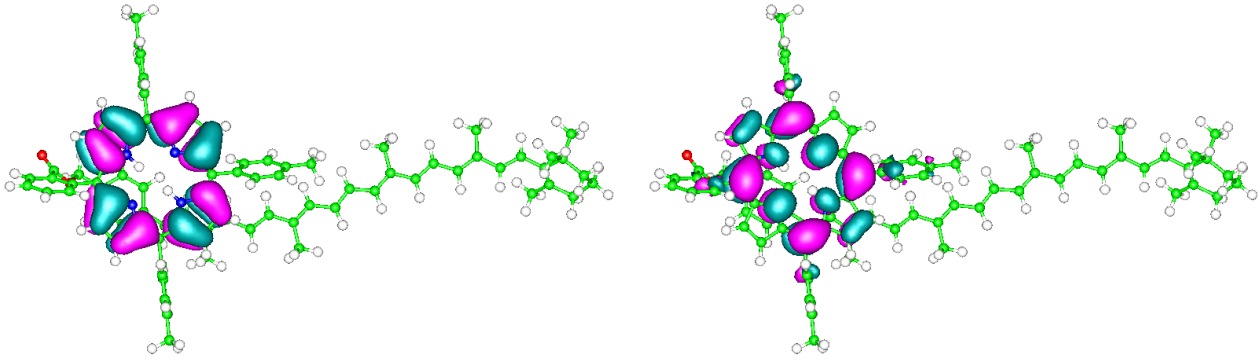

0.37609 0.63766

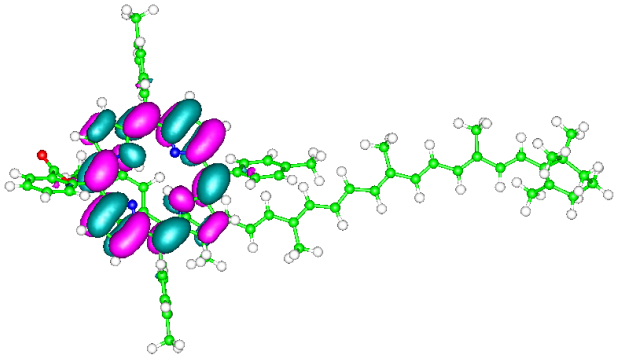

0.63766

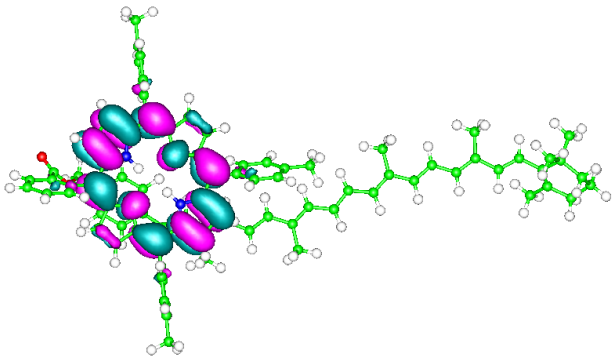

0.37609

$$S_0(Q_{T_1}) \rightarrow S_2(Q_{T_1})$$

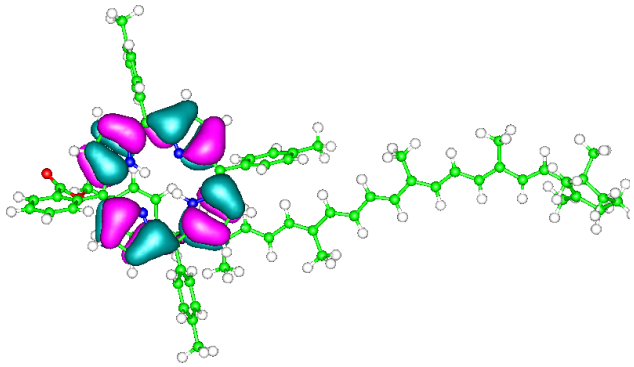

0.37381

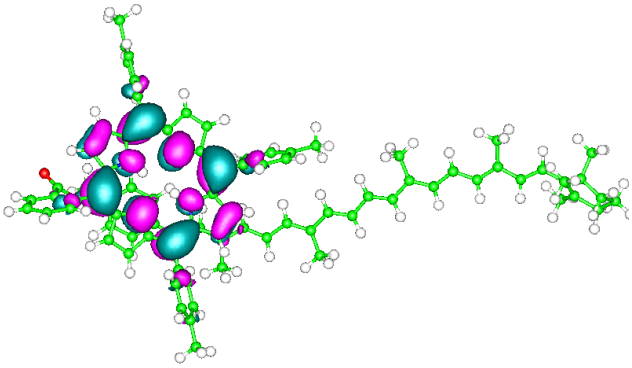

0.63907

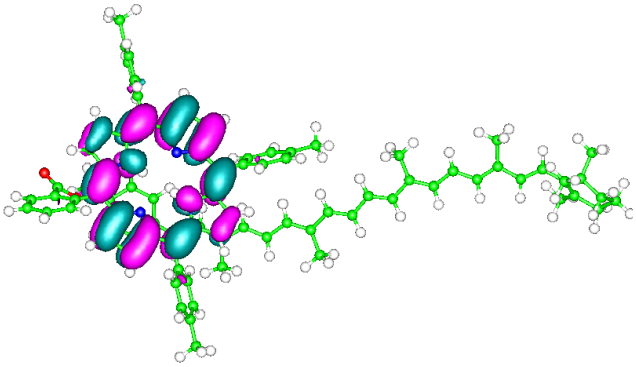

0.63907

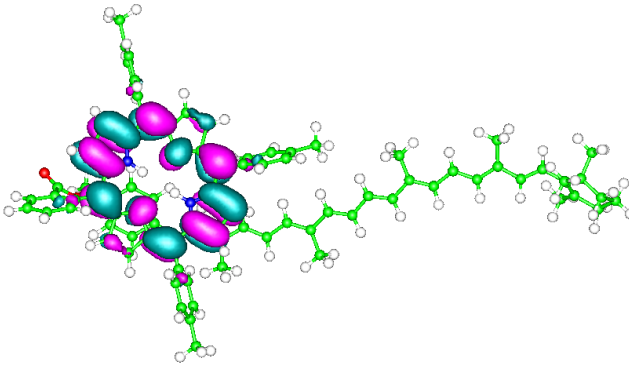

0.37381

$$T_1^{\alpha}(Q_{T_1}) \rightarrow T_2^{\alpha}(Q_{T_1})$$

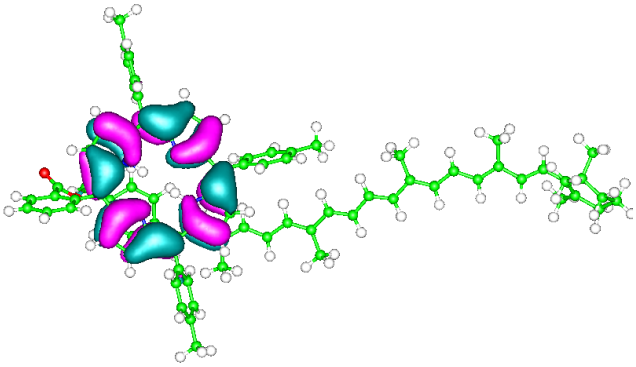

0.36451

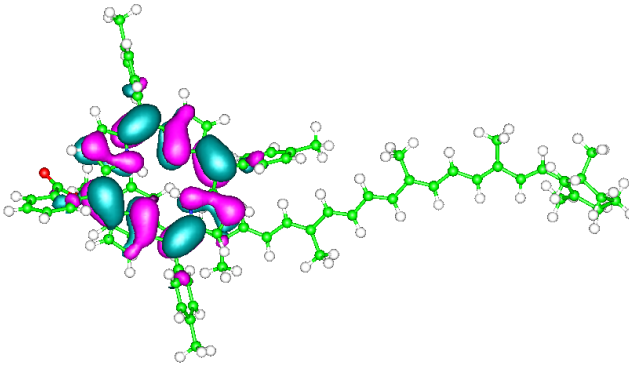

0.66312

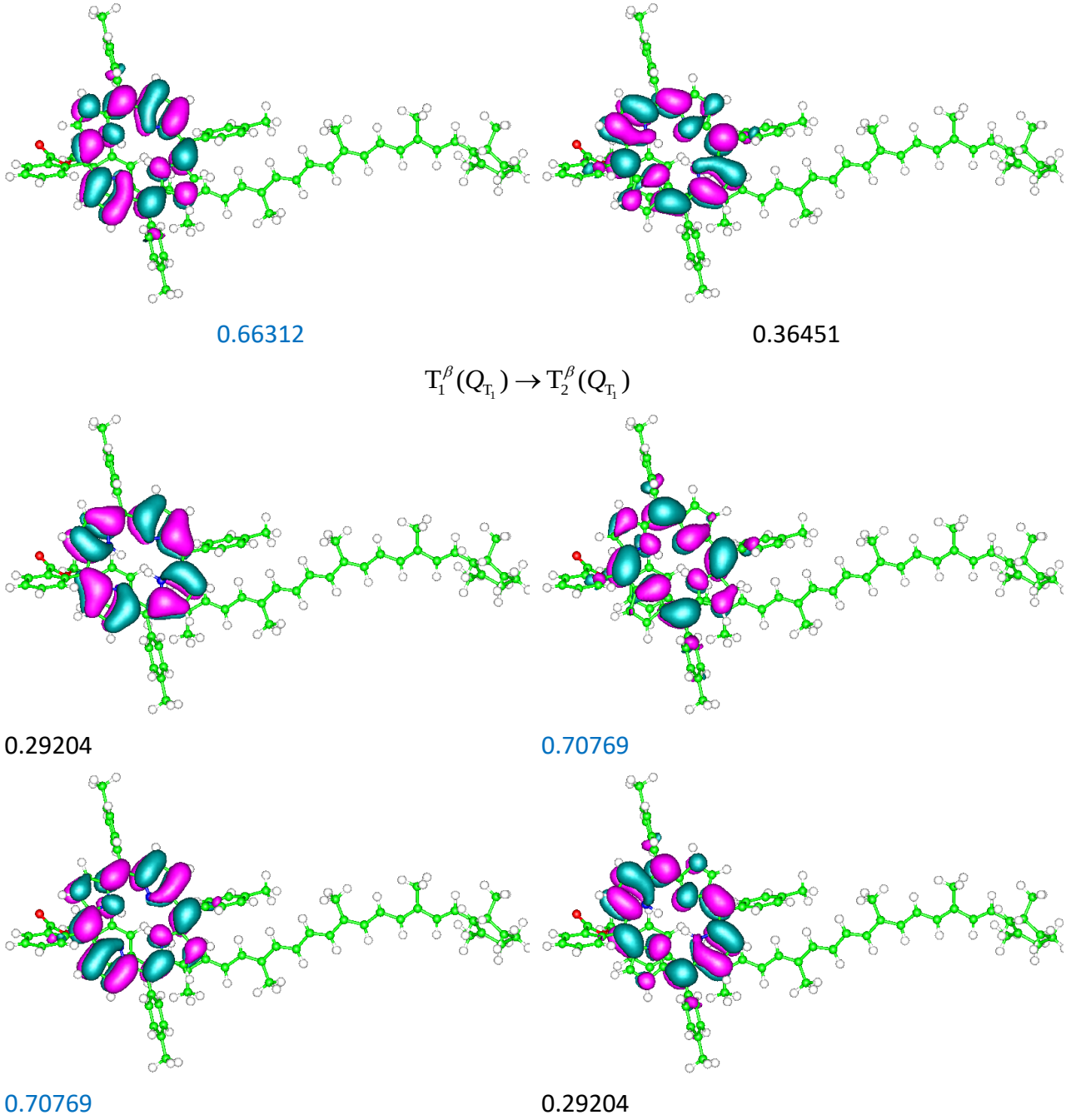

Fig. S3 NTOs most representative of the indicated electronic transitions (and their weights) in the *ortho*-carotenoporphyrin dyad in THF-like solvent. An isovalue of 0.02 is used for the representation. Lobes of different signs are drawn in different color. The weights for the highest occupied and lowest unoccupied NTOs are in blue.

S6. Transition spin density for the $T_1 \rightarrow T_2$ transition in dyad's structure Q_{T_1}

Table S7 Mulliken electron spin density in the T_1 state (which is localized on the carotenoid) and $T_1 \rightarrow T_2$ transition density. The latter is negligible, meaning that the electron density rearrangement does not entail the electron spin density on the carotenoid moiety.

atom	T_1 spin density	$T_1 \rightarrow T_2$ transition spin density
C	-0.079086	0.000188
C	0.094551	-0.000293
C	-0.006605	0.000022
C	0.000892	-0.000004
C	-0.000138	-0.000002
C	0.009911	-0.000022
C	-0.007246	0.000012
H	0.003210	-0.000012
H	0.002473	-0.000015
H	0.001452	-0.000006
H	0.004776	-0.000015
H	-0.000011	-0.000000
H	0.000010	0.000000
H	0.000031	0.000001
H	0.000834	-0.000004
C	-0.001796	0.000007
H	0.000064	-0.000000
H	-0.000211	0.000004
H	0.000298	-0.000000
C	0.000503	-0.000001
H	0.000056	0.000000
H	-0.000199	0.000003
H	0.000229	0.000007
C	0.327686	-0.000217
H	-0.015601	0.000003
C	-0.208535	0.000265
H	0.007669	-0.000010
C	0.448691	0.000196
C	-0.033106	-0.000029
H	0.014389	-0.000007
H	0.015055	-0.000009
H	0.000849	-0.000001
C	-0.294288	-0.000206
H	0.011083	0.000016
C	0.481208	0.000441
H	-0.020935	-0.000028
C	-0.264685	0.000501
H	0.009887	-0.000031
C	0.392175	0.000027
C	-0.028693	-0.000008
H	0.000672	0.000002
H	0.012908	0.000023
H	0.012798	0.000025
C	-0.112306	0.001193

H	0.003639	-0.000057
C	0.203504	-0.001248
H	-0.009734	0.000063
C	0.089250	0.002122
H	-0.004751	-0.000101
C	-0.005786	-0.001922
H	-0.000703	0.000090
C	0.298126	0.001185
C	-0.021788	-0.000097
H	0.009695	0.000025
H	0.010257	0.000026
H	0.000449	0.000002
C	-0.197372	-0.001539
H	0.007389	0.000068
C	0.434374	0.000365
H	-0.018847	-0.000011
C	-0.288009	-0.000805
H	0.011351	-0.000013
C	0.484084	0.002391
C	-0.035214	-0.000208
H	0.009585	0.000034
H	0.019673	0.000154
H	0.003061	0.000019
C	-0.260417	-0.000890
H	0.009786	0.000117
C	0.409833	0.001367
H	-0.018061	-0.000066
C	-0.116431	0.001233
C	0.111655	-0.000844
C	-0.063428	0.000809
C	0.107055	-0.001716
C	-0.064137	0.000804
C	0.102264	-0.001569
H	-0.004302	0.000063
H	0.002331	-0.000029
H	0.002287	0.000016
H	-0.004822	0.000123
C	-0.005027	0.000042
H	0.000158	-0.000011
H	0.001986	0.000027
O	0.002398	0.000307
C	0.000249	-0.000080
O	0.000320	0.000004
C	0.000468	0.001120
C	-0.000011	-0.000285
C	0.000058	0.000807
C	-0.000023	-0.000147
C	0.000099	0.001257
C	-0.000219	-0.002331
H	0.000010	0.000038
H	0.000002	-0.000033
H	0.000004	0.000026
H	-0.000003	-0.000067
C	0.002273	0.018021
C	-0.000820	0.023781
C	0.000976	0.002199
C	-0.000920	0.009536
C	0.001306	0.016561
N	-0.000244	0.010437
C	-0.000622	0.018678
N	0.001038	0.001430

C	-0.001273	-0.004581
C	0.000137	0.008651
C	-0.000451	-0.000652
C	0.002881	-0.001730
C	-0.001190	-0.020040
N	0.000552	-0.006375
C	0.000696	-0.027871
C	-0.000848	-0.003980
C	0.000788	-0.010419
C	-0.003182	0.004299
C	0.001717	0.003809
N	-0.001294	-0.002078
C	0.000478	-0.022042
C	0.002892	0.003207
C	-0.002444	-0.011239
C	-0.001282	-0.011599
C	0.000226	0.001679
C	-0.000222	-0.001063
C	0.000196	0.000173
C	-0.000104	-0.000878
C	0.000147	0.000277
C	-0.000226	-0.000959
C	-0.000010	0.000060
C	-0.000269	0.000235
C	0.000121	-0.000283
C	-0.000061	-0.000302
C	0.000082	-0.000038
C	-0.000050	-0.000049
C	0.000135	0.000168
C	-0.000006	0.000003
C	0.000528	-0.000752
C	0.002005	0.000181
C	0.000135	-0.000250
C	-0.000070	0.000172
C	0.000024	0.000140
C	-0.000093	0.000783
C	0.000019	-0.000014
H	-0.000007	0.000031
H	-0.001497	-0.000134
H	0.000021	-0.000127
H	-0.000080	0.000130
H	-0.000004	-0.000004
H	0.000021	-0.000040
H	0.000699	-0.000003
H	-0.000000	-0.000391
H	0.000005	0.000009
H	-0.000035	-0.000202
H	-0.000008	0.000046
H	0.000034	-0.000488
H	-0.000027	0.000538
H	0.000004	-0.000002
H	0.000033	0.000289
H	0.000073	0.000487
H	-0.000073	-0.000041
H	-0.000005	0.000000
H	0.000000	0.000058
H	0.000004	0.000061
H	-0.000003	-0.000026
H	-0.000011	-0.000021
H	0.000022	-0.000039
H	0.000001	0.000005

H	-0.000004	0.000008
H	-0.000001	0.000001
H	0.000038	-0.000001
H	-0.000088	-0.000031
H	-0.000022	-0.000039
H	0.000001	-0.000001
H	0.000004	-0.000005
H	0.000001	0.000001

S7. Shape dependence of T-S spectra on the Gaussian broadening parameter

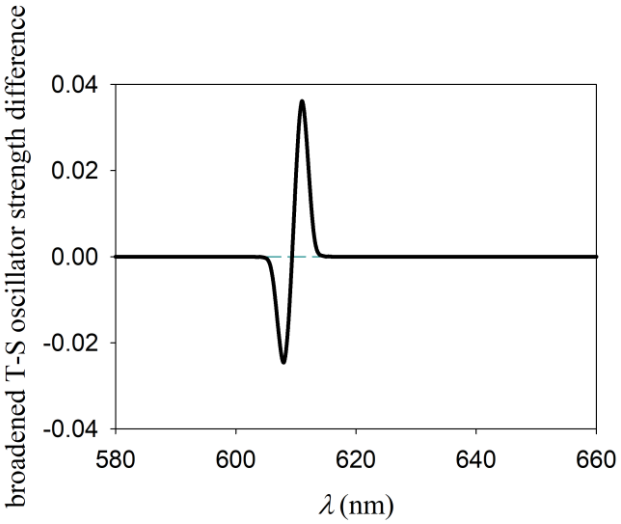

Fig. S4 T-S spectrum as in Fig. 5b but using a Gaussian broadening with a width parameter of 1 nm.

S8. Additional NTOs and excited states for the molecular models from LHCII

In the following tables, the electronic excitations in the relevant spectral range (i.e., with wavelengths relatively close to 650 nm) and with large oscillator strengths are highlighted in blue. The excitations with such properties but characterized by a borderline value of spin contamination (appreciably larger than 10%) are marked in dark gray. TDDFT at the wB97X-D/6-31g* level of computational accuracy is used unless otherwise specified.

Table S8 λ, f and Σ values for the singlet (S) and triplet (T) electronic excitations in the M system surrounded by a PCM with a (relative) dielectric constant typical of protein interiors (p) or THF. The excitations in Table 2 are included.

$\lambda_S^{M,p}$	$f_S^{M,p}$	$\lambda_T^{M,p}$	$f_T^{M,p}$	$\Sigma_T^{M,p}$	$\lambda_S^{M,THF}$	$f_S^{M,THF}$	$\lambda_T^{M,THF}$	$f_T^{M,THF}$	$\Sigma_T^{M,THF}$
652.11	0.7357	2118.50	0.0010	2.145	656.24	0.7637	2127.83	0.0010	2.141
643.19	0.1818	1776.76	0.0410	2.164	645.65	0.2120	1766.78	0.0467	2.168
632.62	0.0859	1605.33	0.0000	4.052	637.65	0.0891	1560.80	0.0000	4.051
530.83	0.0104	1572.66	0.0000	4.051	530.79	0.0120	1546.26	0.0000	4.050
528.45	0.0140	1267.28	0.0000	4.052	527.92	0.0176	1242.62	0.0000	4.051
524.21	0.0169	1051.70	0.0000	4.052	524.92	0.0213	1033.51	0.0000	4.051
432.28	2.2933	1019.54	0.0000	4.051	437.00	2.3956	1014.24	0.0000	4.050
408.93	0.5379	695.81	0.0000	4.052	410.45	0.4603	690.22	0.0000	4.051
396.58	0.0891	684.49	0.0528	2.113	398.31	0.1331	679.51	0.0382	2.205
389.14	0.4828	680.76	0.0086	2.219	394.26	0.6066	675.77	0.0454	2.129
388.91	0.4315	652.96	0.0000	4.052	390.76	1.1673	651.72	0.0000	4.051
385.44	0.2175	644.23	0.4870	2.064	386.58	0.0491	646.69	0.5250	2.060
380.89	0.0283	639.19	0.2704	2.134	383.60	1.2123	642.95	0.2299	2.088
380.41	1.4711	637.28	0.0031	4.024	382.27	0.0071	636.70	0.0152	2.505
367.89	0.6226	634.36	0.0031	2.499	369.18	0.8512	635.33	0.0004	4.035
363.90	1.7837	627.16	0.0491	2.413	365.64	1.9757	626.33	0.0760	2.411
360.74	0.6613	581.37	0.0002	2.076	363.71	0.3422	584.70	0.0001	2.073
354.50	1.2501	563.14	0.0450	2.166	356.70	1.1226	562.52	0.0530	2.164
348.45	0.3580	536.19	0.0000	4.052	351.20	0.3356	532.65	0.0000	4.050
346.64	0.1574	528.44	0.0118	2.052	349.67	0.1438	527.92	0.0136	2.051

For $M_{612} \equiv \{\text{Lut}620, \text{Chl}\,a612\}$, we find only one singlet transition with these properties and no triplet transition with acceptable spin contamination which also has a significant f value (see below). The T_1 state was instead determined with a Σ value well within the acceptance range, that is, 2.05 in both environmental models used. Forcing the electron density to be distributed on M_{612} through a TDDFT

study of the isolated pigment pair changes the electronic structure properties of the transitions to some extent, compared to those occurring in system M, due to the removal of the excitonic coupling effects. In fact, we reach the same conclusion from inspection of the other two pigment pairs contained in M, which stresses the nonnegligible exciton coupling effects in system M.

Table S9 λ, f, and Σ values for the electronic excitations in model system M_{612} surrounded by a PCM with dielectric constants typical of protein interiors (p) and THF solvent.

$\lambda_S^{M_{612},p}$	$f_S^{M_{612},p}$	$\lambda_T^{M_{612},p}$	$f_T^{M_{612},p}$	$\Sigma_T^{M_{612},p}$	$\lambda_S^{M_{612},THF}$	$f_S^{M_{612},THF}$	$\lambda_T^{M_{612},THF}$	$f_T^{M_{612},THF}$	$\Sigma_T^{M_{612},THF}$
634.52	0.2958	2059.44	0.0014	2.139	639.34	0.3170	2086.68	0.0014	2.133
522.83	0.0216	1750.49	0.0306	2.155	523.66	0.0263	1744.19	0.0355	2.162
430.75	2.2302	1267.52	0.0000	4.046	435.42	2.3816	1244.03	0.0000	4.044
408.73	0.6273	695.36	0.0069	2.262	409.80	0.5052	692.06	0.0062	2.208
383.00	1.5602	693.32	0.0001	3.991	388.05	1.7674	688.21	0.0000	4.032
366.29	0.7544	652.69	0.0064	2.135	367.22	0.6861	651.90	0.0070	2.138
349.89	0.9723	641.28	0.0016	2.502	352.97	0.9444	642.14	0.0053	2.500
327.59	0.0043	627.26	0.1680	2.469	327.14	0.0039	623.91	0.1801	2.455
322.80	0.0051	561.58	0.0534	2.147	323.74	0.0040	561.35	0.0621	2.146
317.26	0.0244	514.40	0.0919	2.143	316.82	0.0180	516.06	0.1157	2.121
313.83	0.0107	506.67	0.0010	3.819	315.06	0.0175	504.28	0.0004	3.733
308.37	0.0119	495.02	0.0032	2.309	311.32	0.0110	494.06	0.0040	2.403
297.06	0.1596	473.81	0.2186	2.712	297.05	0.2342	472.83	0.2409	2.708
295.11	0.2198	427.79	1.5536	2.470	295.22	0.1547	431.54	2.5269	2.167
290.79	0.0029	424.66	0.0370	2.352	290.98	0.0030	427.53	0.0024	2.350
286.41	0.0033	420.59	1.7607	2.879	286.30	0.0035	420.83	0.9282	3.102
281.41	0.1101	403.05	0.0513	2.136	281.19	0.1093	403.40	0.0607	2.140
274.63	0.1095	398.70	0.1441	2.254	274.76	0.1081	399.82	0.1344	2.258
270.03	0.0048	390.09	0.4898	2.511	269.96	0.0063	391.51	0.5110	2.510
266.68	0.0756	379.19	0.0696	2.236	266.98	0.0585	381.52	0.0845	2.217

$S_0 \rightarrow S_1$

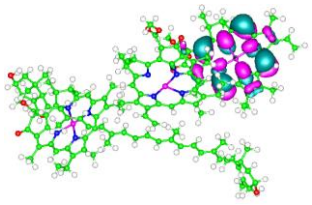
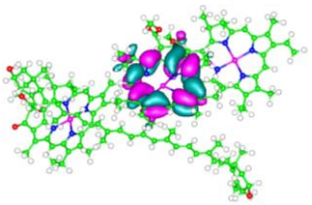
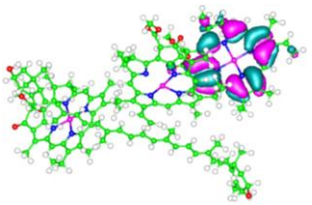

0.08172 0.24339 0.61036

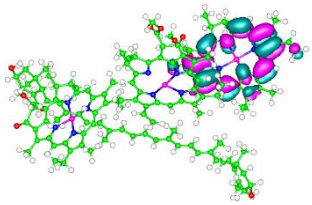
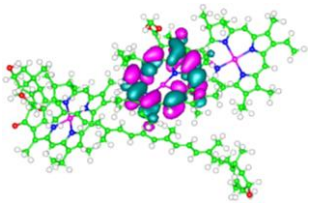
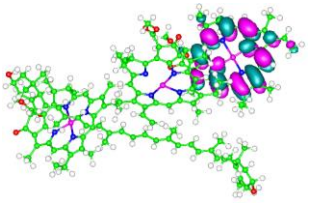

0.61036 0.24339 0.08172

$S_0 \rightarrow S_2$

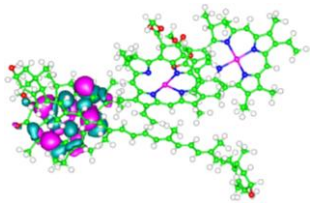
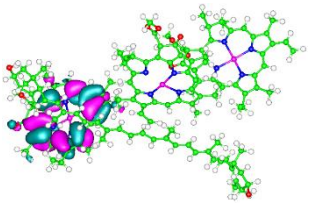
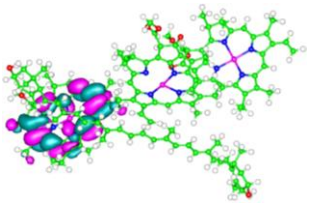
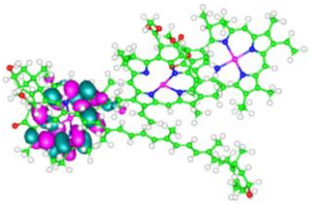

0.12816 0.83537 0.83537 0.12816

$T_1^{\alpha} \rightarrow T_6^{\alpha}$

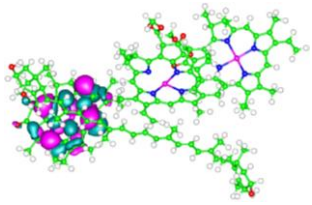
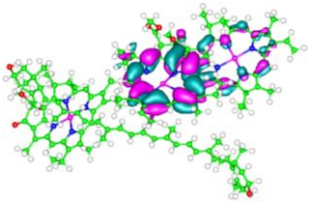
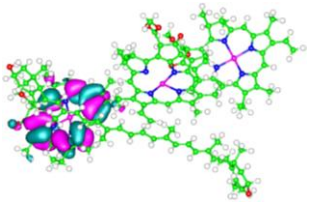

0.10906 0.14853 0.72535

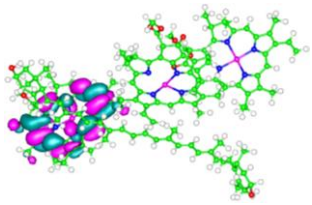
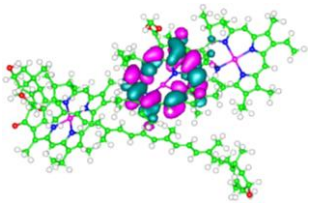
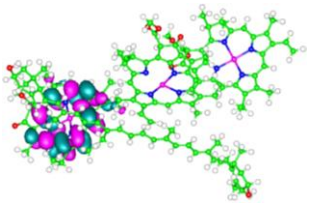

0.72535 0.14853 0.10906

$T_1^{\beta} \rightarrow T_6^{\beta}$

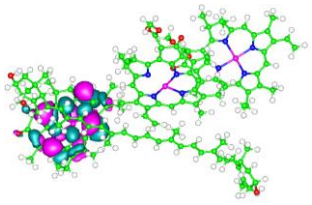
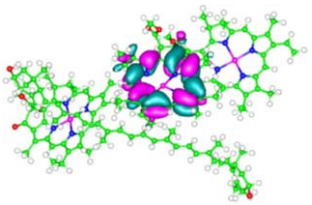
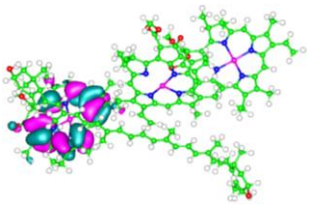

10905 0.11765 0.72535

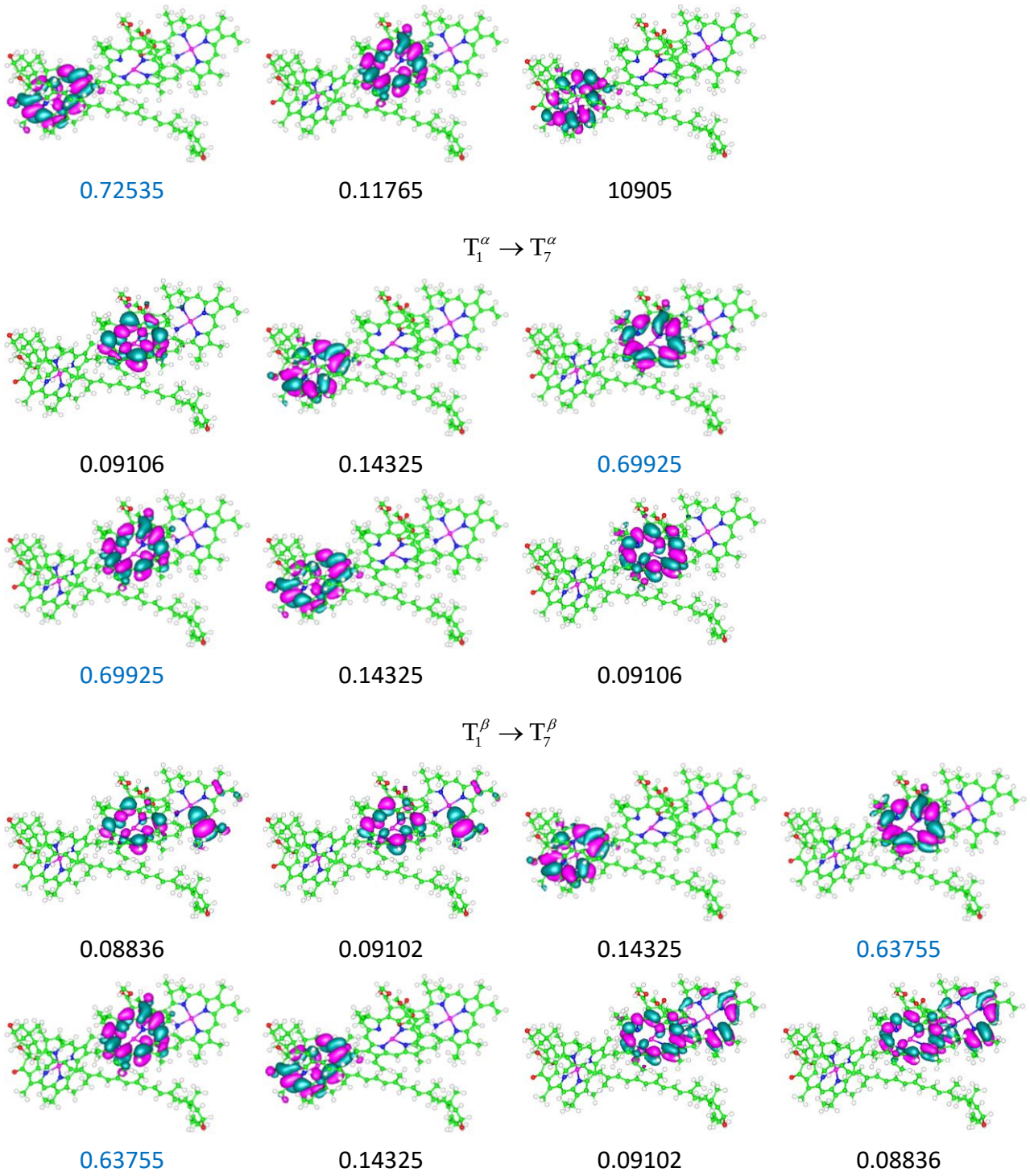

Fig. S5 NTOs most representative of the indicated electronic excitations for the M system in THF (cf. Fig. 7). The weights for the highest occupied and lowest unoccupied NTOs are highlighted in blue. The isovalue 0.02 is shown.

Table S10 λ, f, and Σ values for the electronic excitations in systems M_{612} and M surrounded by a PCM with a dielectric constant typical of solvated-protein surfaces ($\varepsilon_s = 20$ [5]).

$\lambda_S^{M_{612},s}$	$f_S^{M_{612},s}$	$\lambda_T^{M_{612},s}$	$f_T^{M_{612},s}$	$\Sigma_T^{M_{612},s}$	$\lambda_S^{M,s}$	$f_S^{M,s}$	$\lambda_T^{M,s}$	$f_T^{M,s}$	$\Sigma_T^{M,s}$
634.57	0.2984	2116.31	0.0015	2.125	652.04	0.7449	2145.40	0.0008	2.128
524.35	0.0270	1676.35	0.0321	2.168	642.61	0.1858	1685.43	0.0428	2.178
430.94	2.2079	1262.81	0.0000	4.046	632.45	0.0828	1599.02	0.0000	4.053
409.36	0.6434	697.84	0.0061	2.216	531.20	0.0121	1578.19	0.0000	4.052
384.27	1.4866	692.27	0.0000	4.040	529.56	0.0183	1262.30	0.0000	4.053
367.65	0.7689	654.71	0.0058	2.138	525.08	0.0228	1054.02	0.0000	4.053
350.84	0.9862	648.62	0.0020	2.487	432.74	2.2215	1018.74	0.0000	4.052
327.06	0.0031	635.27	0.1842	2.432	410.72	0.6103	694.43	0.0000	4.053
318.77	0.0289	562.27	0.0608	2.154	396.22	0.0758	688.42	0.0417	2.205
317.02	0.0059	511.48	0.0967	2.136	391.92	0.2489	684.61	0.0458	2.143
313.55	0.0101	505.72	0.0012	3.904	389.95	0.5862	652.26	0.0000	4.053
308.34	0.0113	491.32	0.0020	2.218	387.45	0.1838	646.40	0.0042	2.503
298.88	0.0506	479.30	0.1820	2.779	383.41	0.0060	644.49	0.5982	2.120
296.61	0.3740	427.97	1.4610	2.521	381.68	1.3713	640.81	0.1246	2.164
291.27	0.0030	421.11	1.8838	2.857	369.77	0.4983	635.37	0.0010	4.042
287.19	0.0050	412.64	0.0155	2.329	365.77	1.7447	632.62	0.0791	2.244
281.41	0.1167	404.32	0.0503	2.135	362.27	0.7158	589.85	0.0001	2.076
277.48	0.1113	400.46	0.1260	2.244	355.47	1.4355	563.20	0.0499	2.169
270.02	0.0036	390.59	0.4768	2.509	350.08	0.4303	540.08	0.0000	4.053
267.77	0.0351	382.27	0.0743	2.244	347.40	0.1354	529.56	0.0160	2.053

$S_0 \rightarrow S_1$

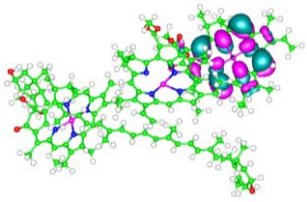
0.08449

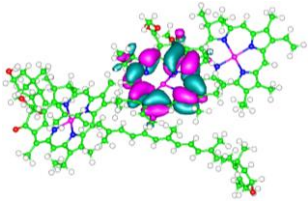
0.23653

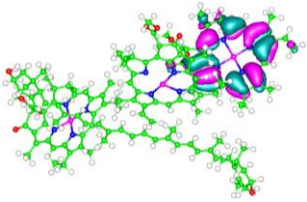
0.59806

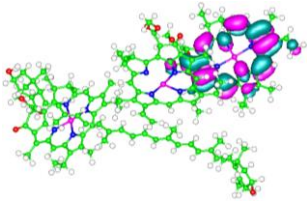
0.59806

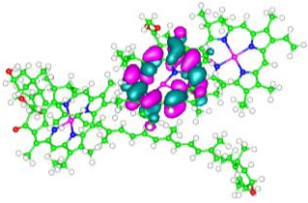
0.23653

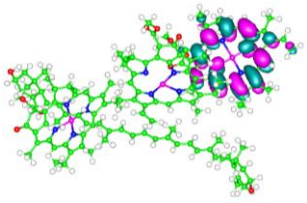
0.08449

$S_0 \rightarrow S_2$

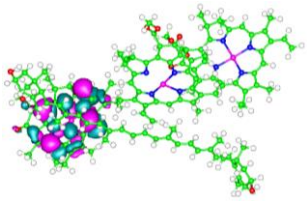
13266

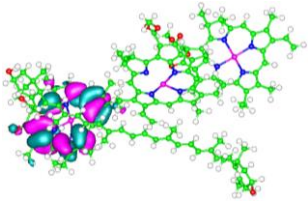
0.81524

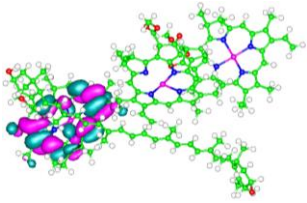
0.81524

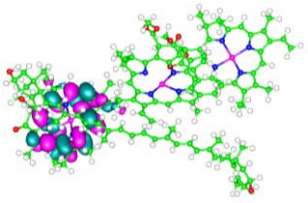
13266

$T_1^{\alpha} \rightarrow T_6^{\alpha}$

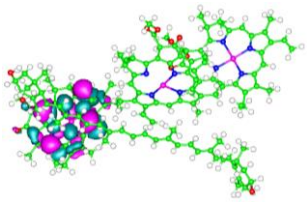
0.08466

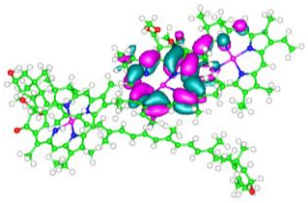
0.09566

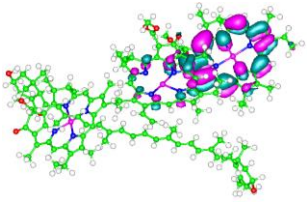
0.41093

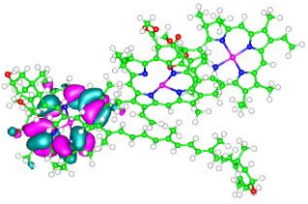
0.53784

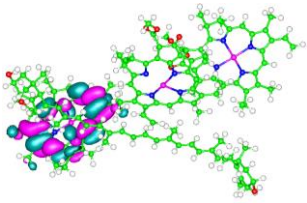
0.53784

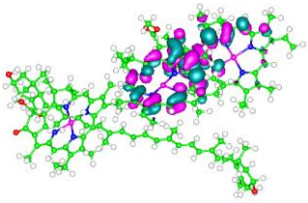
0.41093

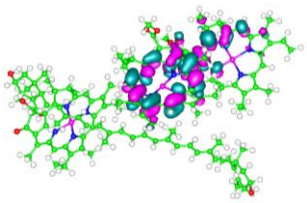
0.09566

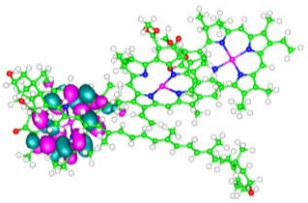
0.08466

$T_1^{\beta} \rightarrow T_6^{\beta}$

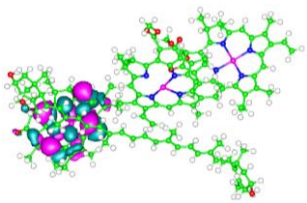
0.08466

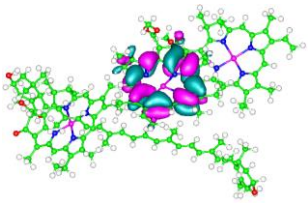
0.13115

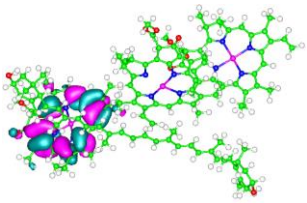
0.53778

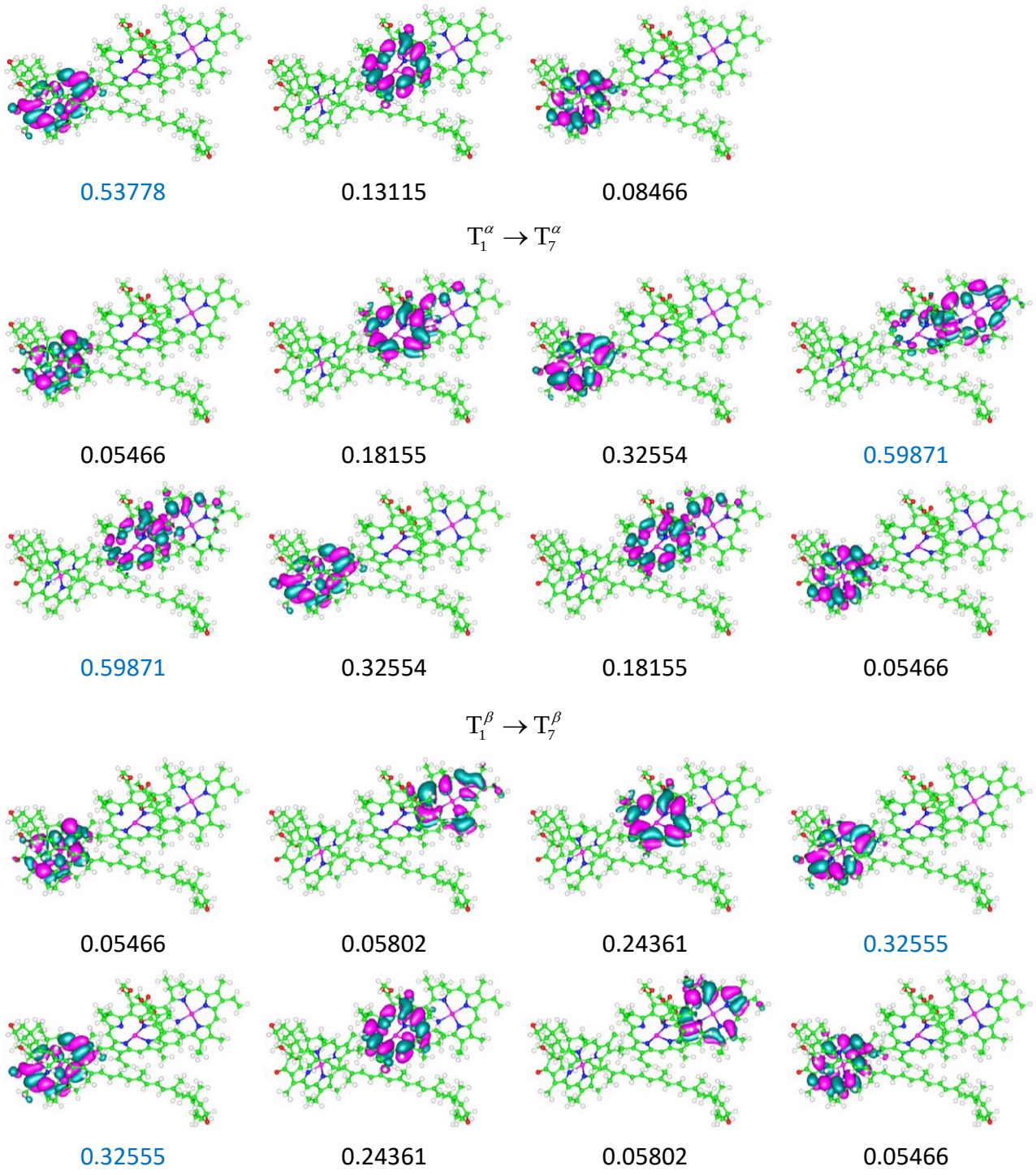

Fig. S6 The analogue of Fig. S5 for the M system in a PCM modeling solvated-protein surfaces.

Table S11 λ, f, and Σ values for the electronic excitations in systems M_{612} and M in vacuum.

$\lambda_S^{M_{612},v}$	$f_S^{M_{612},v}$	$\lambda_T^{M_{612},v}$	$f_T^{M_{612},v}$	$\Sigma_T^{M_{612},v}$	$\lambda_S^{M,v}$	$f_S^{M,v}$	$\lambda_T^{M,v}$	$f_T^{M,v}$	$\Sigma_T^{M,v}$
622.69	0.2125	2034.82	0.0044	2.202	640.24	0.5723	2117.90	0.0055	2.207
520.25	0.0089	1835.18	0.0168	2.097	630.89	0.1396	1871.95	0.0241	2.109
419.36	1.5943	1276.56	0.0000	4.045	621.62	0.0493	1608.25	0.0000	4.051
401.96	0.8539	695.42	0.0000	4.044	528.47	0.0044	1567.46	0.0000	4.051
370.79	1.1963	685.87	0.0061	2.214	525.52	0.0049	1275.43	0.0000	4.051
357.22	1.0852	639.99	0.0046	2.137	521.73	0.0063	1046.38	0.0000	4.051
341.63	0.8547	625.67	0.0011	2.500	422.22	1.6660	1021.05	0.0000	4.051
335.10	0.0162	610.21	0.0904	2.567	403.57	0.6896	697.97	0.0000	4.051
330.72	0.0265	560.24	0.0334	2.146	399.70	0.0168	694.52	0.0125	2.082
315.13	0.0277	518.98	0.0440	2.187	379.43	0.2624	672.79	0.0094	2.239
311.94	0.0145	511.65	0.0067	2.679	376.37	0.4293	654.97	0.0000	4.051
298.99	0.0148	503.92	0.0013	3.444	373.91	0.0180	639.89	0.0001	4.050
295.74	0.2088	457.70	0.1192	2.486	373.55	0.1985	632.11	0.3948	2.065
288.36	0.0523	455.50	0.0919	2.473	369.38	0.9763	628.32	0.1800	2.082
287.65	0.0030	422.70	0.1750	3.037	360.59	0.5071	617.33	0.0090	2.471
285.05	0.0420	410.06	2.6384	2.300	355.45	2.2442	610.98	0.0259	2.569
280.72	0.1037	396.98	0.0476	2.139	353.44	0.2562	562.67	0.0185	2.143
269.70	0.0050	395.62	0.2936	2.236	347.71	1.1795	557.96	0.0104	2.106
269.00	0.0990	384.96	0.3400	2.520	341.28	0.4131	530.62	0.0000	4.051
264.45	0.0947	378.53	0.0001	4.044	338.69	0.1874	525.58	0.0060	2.066

$S_0 \rightarrow S_1$

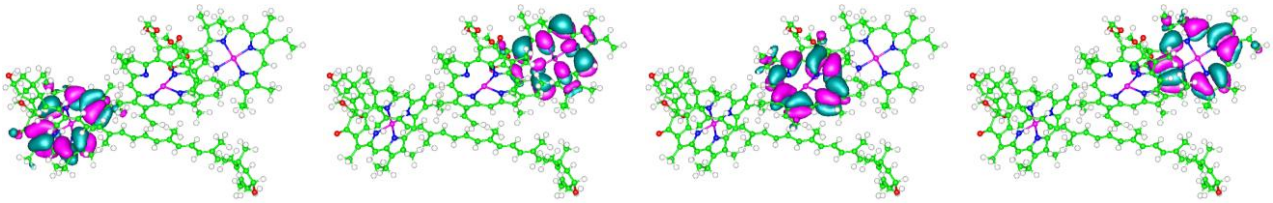

0.05576 0.09201 0.26412 0.54504

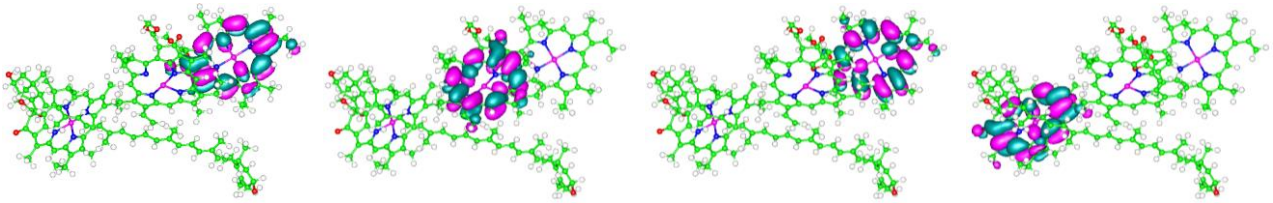

0.54504 0.26412 0.09201 0.05576

$S_0 \rightarrow S_2$

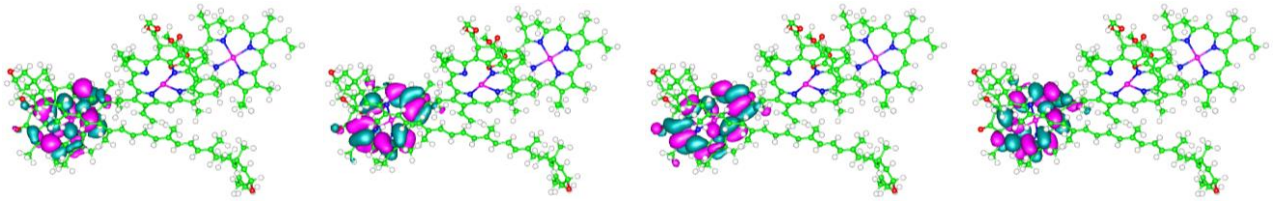

0.15009 0.78806 0.78806 0.15009

$T_1^{\alpha} \rightarrow T_6^{\alpha}$

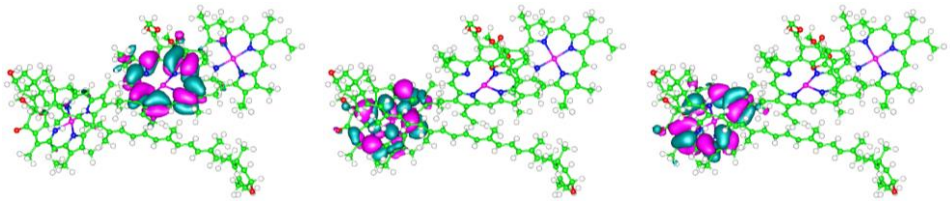

0.12763 0.13001 0.69906

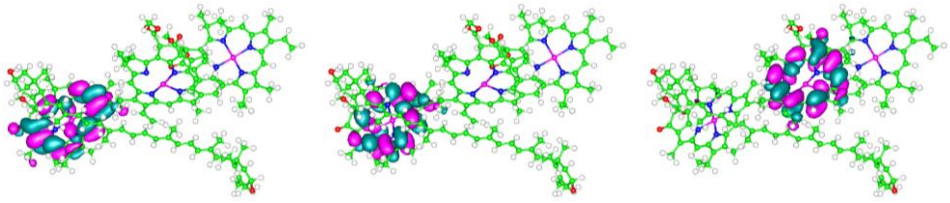

0.69906 0.13001 0.12763

$T_1^{\beta} \rightarrow T_6^{\beta}$

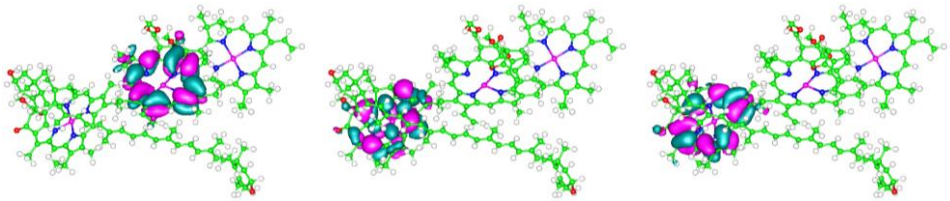

0.12135 0.12995 0.69906

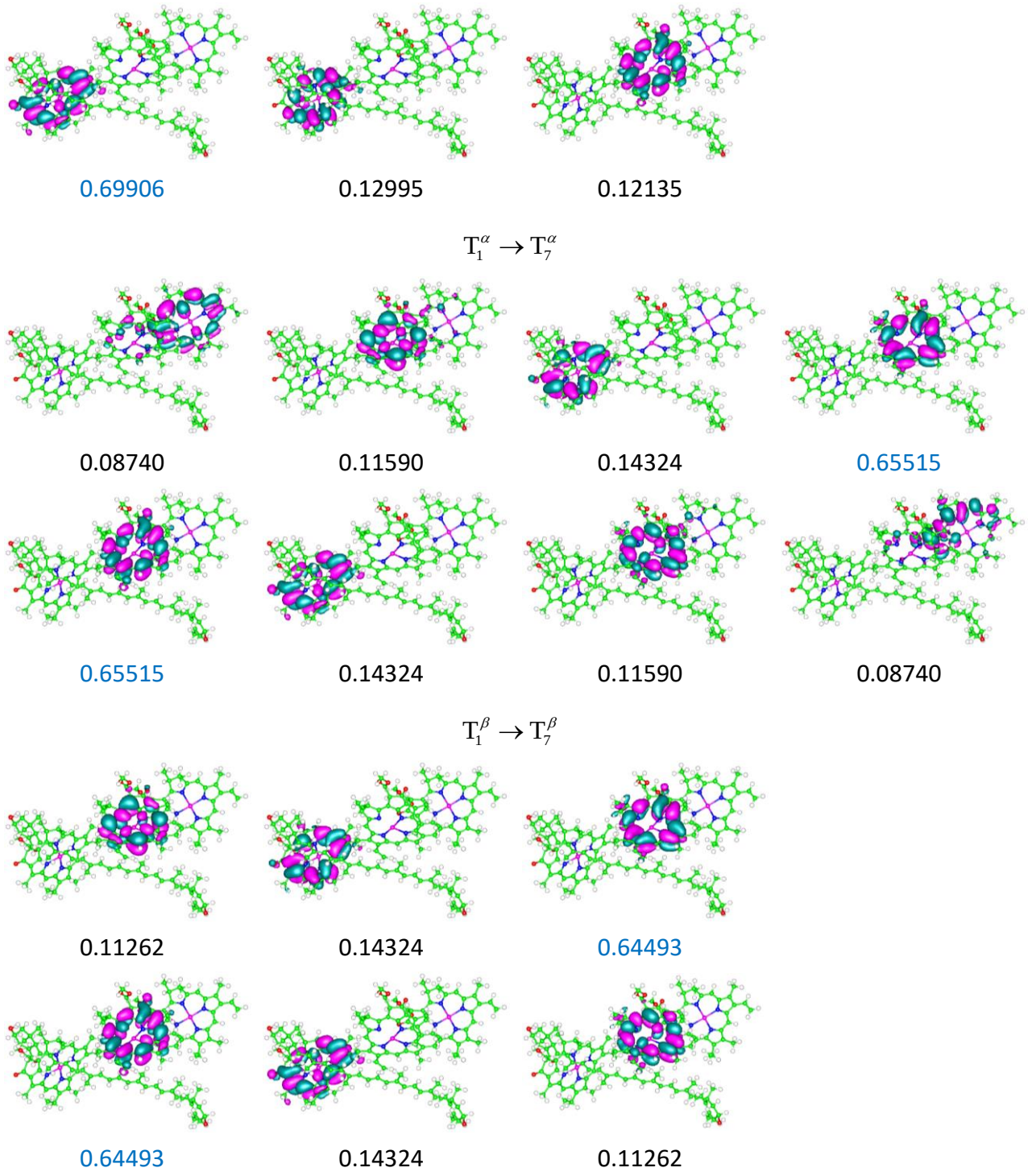

Fig. S7 The analogue of Fig. S5 for the M system in vacuum.

Table S12 λ, f and Σ values for the singlet (S) and triplet (T) electronic excitations in the M' and M″ systema surrounded in protein interior-like environment. The excitations in Table 3 are included.

$\lambda_p^{M',S}$	$f_p^{M',S}$	$\lambda_p^{M',T}$	$f_p^{M',T}$	$\Sigma_p^{M',T}$	$\lambda_p^{M'',S}$	$f_p^{M'',S}$	$\lambda_p^{M'',T}$	$f_p^{M'',T}$	$\Sigma_p^{M'',T}$
864.01	3.1355	1626.86	0.0000	4.215	902.90	2.8464	1626.30	0.0000	4.220
693.72	0.0277	1605.22	0.0000	4.194	693.07	0.3536	1582.57	0.0000	4.218
651.30	0.6619	1602.96	0.0000	4.215	650.03	0.6438	1571.19	0.0000	4.208
642.50	0.2117	1088.34	0.0000	4.215	646.26	0.0974	1088.25	0.0000	4.220
632.77	0.0704	1047.38	0.0000	4.209	628.11	0.0897	1052.42	0.0000	4.218
543.05	0.0752	1044.26	0.0000	4.215	603.70	0.0084	1018.31	0.0001	4.202
542.33	0.0009	784.16	0.0051	2.767	531.28	0.0078	758.06	0.0246	2.756
530.69	0.0186	707.51	0.0046	4.020	529.79	0.0117	652.90	0.4599	2.973
527.48	0.0117	656.60	0.4263	2.318	528.48	0.0103	652.54	0.2505	3.457
469.15	0.0161	653.01	0.0000	4.214	489.81	0.0808	646.01	0.0026	3.887
452.10	0.0218	644.72	0.0000	4.215	459.39	0.0819	645.18	0.0000	4.219
441.82	0.0661	644.06	0.4673	2.277	451.79	0.0292	643.71	0.1983	2.235
422.77	0.0132	641.35	0.0269	2.243	445.09	0.0055	633.96	0.0660	2.235
421.35	0.0036	616.60	0.0849	2.404	442.77	0.0104	603.80	0.0097	2.699
415.72	0.0028	543.93	0.0691	2.263	424.61	0.0020	538.01	0.0036	2.376
408.47	0.3181	541.87	0.0002	4.005	406.35	0.0156	533.63	0.0000	4.088
408.24	0.5537	537.45	0.0030	4.076	394.98	0.1909	530.89	0.0102	2.220
396.05	0.4667	530.70	0.0264	2.248	390.42	0.5680	529.51	0.0000	4.220
392.51	0.0611	530.49	0.0053	2.440	389.63	0.2457	528.33	0.0294	2.230
390.25	0.2439	529.04	0.0000	4.215	388.47	0.0137	523.19	0.0049	2.276

Table S13 Properties of the singlet excited states in structure M, obtained using the M06-2X density functional. Units are as in the other tables. The excitations in Table 3 are included.

$\lambda_p^{M,S}$	$f_p^{M,S}$
621.48	0.7981
612.11	0.2211
604.44	0.0804
515.95	0.0083
514.15	0.0145
512.29	0.0107
473.13	0.1935
458.95	0.0034
446.94	0.0014
441.47	0.0500
433.60	2.5675
412.27	0.0014
406.16	0.0007
392.85	0.1230
391.84	0.0954
389.17	0.5415
385.02	0.1979
384.95	0.3195
382.80	0.0010
381.49	1.3938

Table S14 We report the same quantities as in Table S12 obtained using the M06-2X functional. The excitations in Table 3 are included.

$\lambda_p^{M',S}$	$f_p^{M',S}$	$\lambda_p^{M',T}$	$f_p^{M',T}$	$\Sigma_p^{M',T}$	$\lambda_p^{M'',S}$	$f_p^{M'',S}$	$\lambda_p^{M'',T}$	$f_p^{M'',T}$	$\Sigma_p^{M'',T}$
842.03	2.8502	1055.16	0.0000	4.098	891.66	2.2715	1054.56	0.0000	4.101
792.19	0.2572	1045.05	0.0000	4.097	799.30	0.6320	1041.91	0.0000	4.098
677.69	0.0049	1024.71	0.0004	3.942	743.29	0.0397	1041.39	0.0000	4.079
624.33	0.6830	885.17	0.0019	3.393	623.37	0.7925	831.04	0.0044	2.710
611.97	0.3554	832.54	0.0020	3.080	617.62	0.0010	794.85	0.0000	4.100
608.45	0.0173	794.63	0.0000	4.098	613.40	0.2733	784.14	0.0001	4.079
576.83	0.0001	779.77	0.0000	4.090	607.82	0.0163	773.85	0.0378	2.519
537.57	0.0523	763.67	0.0507	2.300	554.68	0.0462	762.27	0.0082	3.394
534.90	0.0029	692.47	0.0020	2.152	531.26	0.0137	721.17	0.0143	2.171
530.11	0.0051	638.61	0.0049	3.997	522.59	0.0016	622.95	0.7553	2.107
515.72	0.0147	623.06	0.6541	2.112	516.01	0.0080	613.44	0.2521	2.126
513.59	0.0116	611.84	0.3707	2.101	513.46	0.0191	611.87	0.0012	2.162
498.23	0.0008	608.09	0.0015	4.061	510.00	0.0131	608.40	0.0029	4.072
492.69	0.0481	607.75	0.0366	2.133	505.92	0.1086	606.76	0.0332	2.169
486.78	0.0008	600.52	0.0000	4.098	490.31	0.0218	600.99	0.0000	4.100
468.88	0.0018	590.71	0.0222	2.183	465.73	0.0011	600.50	0.0143	3.685
454.32	0.0070	586.01	0.0010	2.141	451.91	0.0224	589.25	0.0393	2.246
454.17	0.0013	563.03	0.4601	2.306	450.89	0.0040	539.15	0.2901	2.250
439.17	0.0020	539.79	0.0142	2.237	447.46	0.0021	526.10	0.2613	2.282
413.72	0.0156	529.08	0.6616	3.246	435.37	0.0002	515.92	0.0284	2.102

Table S15 Excitation energies in the $M_{612} \equiv \{\text{Lut620}, \text{Chl}\,a612\}$ subsystem drawn from M and M″, in protein interior-like environment.

$\lambda^{M,S}_{M_{612}}$	$f^{M,S}_{M_{612}}$	$\lambda^{M,T}_{M_{612}}$	$f^{M,T}_{M_{612}}$	$\langle S^2 \rangle^{M,T}_{M_{612}}$	$\lambda^{M'',S}_{M_{612}}$	$f^{M'',S}_{M_{612}}$	$\lambda^{M'',T}_{M_{612}}$	$f^{M'',T}_{M_{612}}$	$\langle S^2 \rangle^{M'',T}_{M_{612}}$
634.52	0.2958	2059.44	0.0014	2.139	887.45	2.8758	1566.06	0.0000	4.209
522.83	0.0216	1750.49	0.0306	2.155	689.75	0.2807	1016.81	0.0001	4.202
430.75	2.2302	1267.52	0.0000	4.046	628.07	0.2167	755.78	0.0226	2.760
408.73	0.6273	695.36	0.0069	2.262	528.78	0.0045	645.58	0.0032	3.841
383.00	1.5602	693.32	0.0001	3.991	488.61	0.0992	636.46	0.2805	2.253
366.29	0.7544	652.69	0.0064	2.135	455.04	0.1443	605.05	0.0134	2.738
349.89	0.9723	641.28	0.0016	2.502	440.39	0.0112	534.81	0.0028	3.828
327.59	0.0043	627.26	0.1680	2.469	405.07	0.0466	532.14	0.0096	2.659
322.80	0.0051	561.58	0.0534	2.147	385.81	0.4968	521.31	0.0180	2.257
317.26	0.0244	514.40	0.0919	2.143	382.65	0.4350	506.00	0.0001	4.103
313.83	0.0107	506.67	0.0010	3.819	367.55	0.6667	467.71	2.6591	2.326
308.37	0.0119	495.02	0.0032	2.309	345.90	0.9857	448.02	0.1522	2.734
297.06	0.1596	473.81	0.2186	2.712	329.96	0.0071	429.42	0.0760	2.388
295.11	0.2198	427.79	1.5536	2.470	327.59	0.0051	421.42	0.4208	2.456
290.79	0.0029	424.66	0.0370	2.352	323.85	0.1787	392.67	0.0029	4.168
286.41	0.0033	420.59	1.7607	2.879	322.34	0.0104	386.46	0.2011	3.068
281.41	0.1101	403.05	0.0513	2.136	319.30	0.0226	381.48	0.9290	2.419
274.63	0.1095	398.70	0.1441	2.254	299.78	0.0947	380.18	0.0070	4.118
270.03	0.0048	390.09	0.4898	2.511	296.84	0.0826	375.23	0.0427	2.480
266.68	0.0756	379.19	0.0696	2.236	296.19	0.7483	370.88	0.0967	3.368

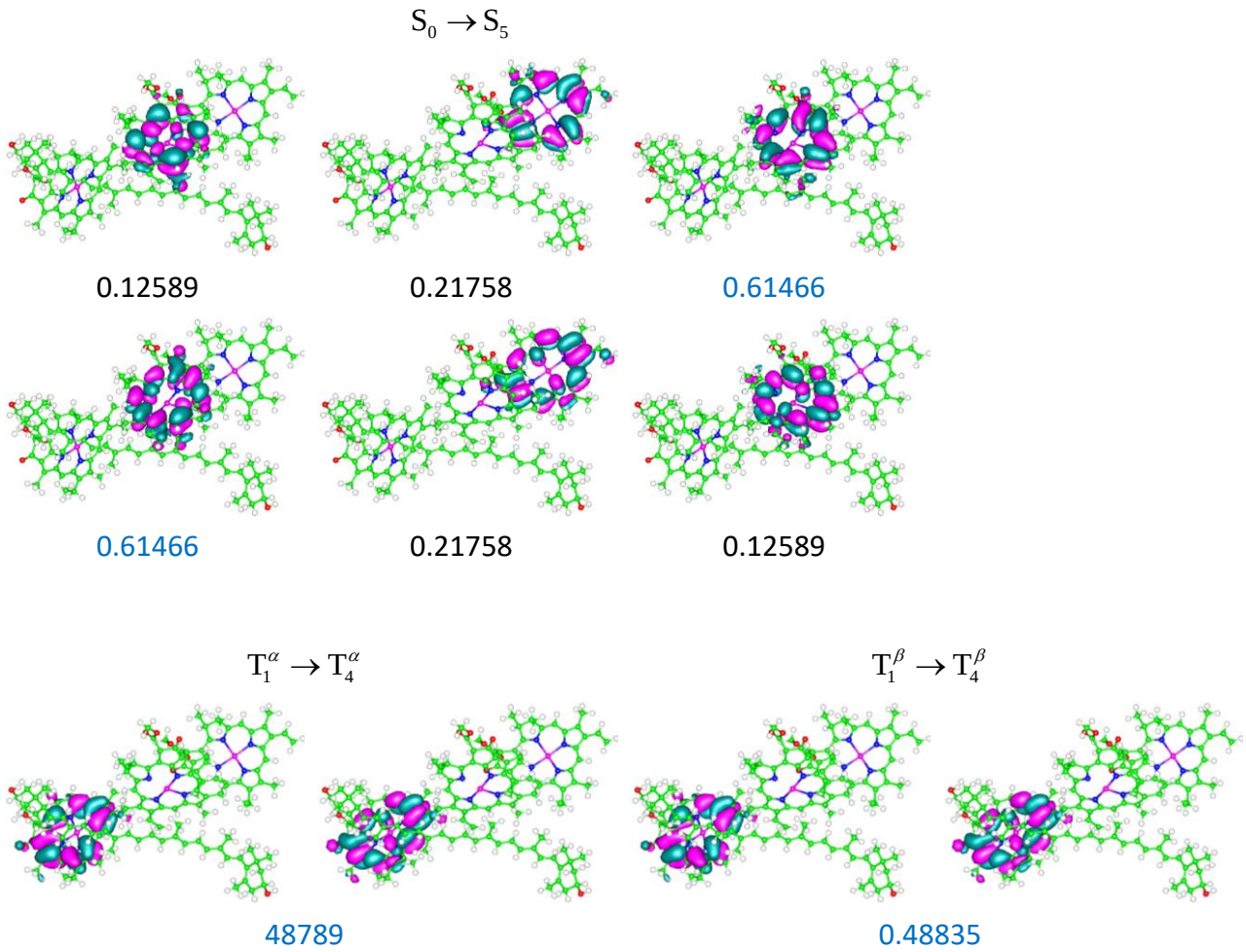

Fig. S8 NTOs representative of the $S_0 \rightarrow S_5$ and $T_1 \rightarrow T_4$ transitions in M' in protein interior-like environment.

S9. Properties of the singlet transitions

Ref. 6 reports on-site excitation energies of 14944, 14876 and 15141 cm^{-1} for Chls *a*610, 611 and 612, respectively. These values were obtained using the QM/MMpol[7] method with the M06-2X functional and the 6-31+G(d) basis set. Moreover, the site energies were shifted by –1210 cm^{-1}. Using the $S_0 \rightarrow S_1$ excitation energy of Chl *a*611 as the zero of the energy scale, the corresponding excitations in Chl *a*610 and Chl *a*612 are 68 and 265 cm^{-1}, respectively. These relative values of the excitation energies are consistent with the NTOs shown in Figs. 7-9. In fact, the electronic excitations $S_0 \rightarrow S_3$, $S_0 \rightarrow S_4$, and $S_0 \rightarrow S_5$ mainly occur on Chls *a*611, *a*610, and *a*612, respectively. We calculated the on-site

excitation energies of the three chlorophylls using their geometries in system M (or, equivalently, in M' and M″, as the chlorophylls were fixed in the geometry optimizations leading to these structures). We used the wB97X-D/6-31g* and M06-2X/6-31+g* computational setups in the continuum model of a protein interior. Both approaches confirm the site energy trend obtained in ref. 6 using a different theoretical method, which also supports the results found in this study by describing the environment as a PCM (see Table S16)

Table S16 Site excitation energy of Chl *a*611 and relative excitation energies of Chl *a*610 and Chl *a*611 expressed in cm^{-1}. 1210 cm^{-1} was added back to the value for Chl *a*611 from ref. 6 to enable the comparison.

Method	*E* (Chl *a*611)	Δ*E* (Chl *a*610)	Δ*E* (Chl *a*612)
QM/MMpol,[7] M06-2X/6-31+g* (ref. 6)	16086	68	265
TDDDFT-SCRF, M06-2X/6-31+g*	15986	100	210
TDDDFT-SCRF, ωB97X-D/6-31g*	15534	100	186
TDDDFT, ωB97X-D/6-31g*	15891	92	178

The relevant $S_0 \rightarrow S_3$, $S_0 \rightarrow S_4$, and $S_0 \rightarrow S_5$ excitations studied in different molecular systems are clearly identified with the excitations $S_0 \rightarrow S_1(Q_y)$, each mainly localized on one of the chlorophylls. This is shown in Table S17 (to be compared with the Tables 1 and 2 in ref. 8).

Table S17 Properties of the indicated singlet electronic excitations, including their excitation energy *E*, the corresponding wavelength λ, the dipole oscillator strength *f*, the major MOs involved, and the absolute values of the corresponding coefficients in the linear combinations describing the electronic excitations. Only the MO excitations with contributions larger than 0.2 are reported. The largest MO contributions to the excitations are highlighted in blue. The approximate correspondence between the MOs in M″ and in the isolated chlorophylls is shown in parentheses.

system	excitation	E (eV)	λ (nm)	f	main MOs involved	MO contributions
Chl *a*610	$S_0 \rightarrow S_1$	1.94	639.63	0.30	HOMO → LUMO	0.65
					HOMO – 1 → LUMO + 1	0.26
Chl *a*611	$S_0 \rightarrow S_1$	1.93	643.76	0.31	HOMO → LUMO	0.66
					HOMO – 1 → LUMO + 1	0.25
Chl *a*612	$S_0 \rightarrow S_1$	1.95	635.16	0.30	HOMO → LUMO	0.65
					HOMO – 1 → LUMO + 1	0.25
M″	$S_0 \rightarrow S_3$	1.91	650.03	0.64	HOMO – 2 → LUMO + 2 ($HOMO_{a610} \rightarrow LUMO_{a610}$)	0.32
					HOMO – 1 → LUMO + 1 ($HOMO_{a611} \rightarrow LUMO_{a611}$)	0.41
					HOMO – 1 → LUMO + 3 ($HOMO_{a611} \rightarrow LUMO_{a612}$)	0.32
	$S_0 \rightarrow S_4$	1.92	646.26	0.10	HOMO – 2 → LUMO + 2 ($HOMO_{a610} \rightarrow LUMO_{a610}$)	0.54
					HOMO – 1 → LUMO + 1 ($HOMO_{a611} \rightarrow LUMO_{a611}$)	0.23
	$S_0 \rightarrow S_5$	1.97	628.11	0.09	HOMO – 3 → LUMO + 1 ($HOMO_{a612} \rightarrow LUMO_{a611}$)	0.30
					HOMO – 3 → LUMO + 3 ($HOMO_{a612} \rightarrow LUMO_{a612}$)	0.43
					HOMO – 1 → LUMO + 1 ($HOMO_{a611} \rightarrow LUMO_{a611}$)	0.24

The study in ref. 8 finds that the first Q_y transition mainly amounts to the HOMO → LUMO transition. We consistently find that the $S_0 \rightarrow S_1$ transition in each isolated chlorophyll mainly involves a HOMO → LUMO transition. Furthermore, the excitation energies obtained in this study are very close to the quasi-experimental values used as reference values in ref. 8. Table S17 shows exciton coupling effects through the combinations of MOs localized on different chlorophylls that describe the transitions and the fact that the $S_0 \rightarrow S_3$ and $S_0 \rightarrow S_4$ excitations are lower in energy than the $S_0 \rightarrow S_1$ excitations in the isolated chlorophylls, compatibly with the coupling values calculated in ref. 6.

S10. Atomic coordinates of the M, M' and M″ systems

Nuclear coordinates of system M (the H atoms, including those used to saturate the pruned molecular system, were optimized as described in the paper, while the coordinates of the heavy atoms are as in the crystal structure from the PDB file 1RWT[9]):

Mg	2.16400000	27.50600100	116.34700000
C	3.88400000	28.50099900	119.23000300
C	-0.74400000	28.72900000	117.72399900
C	0.72000000	27.33099900	113.26100200
C	5.19200000	26.48200000	115.03900100
N	1.63100000	28.41099900	118.23100300
C	2.50800000	28.84199900	119.21900200
C	1.72300000	29.61500000	120.26899700
C	0.31100000	29.15800100	120.04100000
C	0.33200000	28.69899900	118.59500100
C	-0.08700000	27.97200000	120.94100200
C	1.90700000	31.15500100	120.15899700
N	0.35200000	28.05400100	115.60299700
C	-0.73300000	28.45200000	116.35399600
C	-1.88200000	28.57099900	115.48999800
C	-1.48200000	28.26700000	114.22200000
C	-0.07500000	27.85800000	114.30500000
C	-3.27600000	28.99300000	116.04599800
C	-2.51900000	28.44700100	113.20700100
C	-2.39300000	28.17100000	111.89600400
N	2.83500000	26.93300100	114.48799900
C	2.07000000	26.91099900	113.33899700
C	2.87400000	26.38600000	112.24900100
C	4.14300000	26.23100100	112.72300000
C	4.11100000	26.54299900	114.13999900
C	2.47600000	26.10600100	110.79200000
C	5.40900000	25.78599900	111.92199700
C	6.13900000	26.87000100	111.12799800
N	4.02800000	27.19700100	117.06800100
C	5.16800000	26.78700100	116.41400100
C	6.30200000	26.77800000	117.33400000
C	5.84800000	27.40500100	118.45900000
C	4.47000000	27.71600000	118.25199900
C	7.68900000	26.22200000	117.09100300
C	6.20300000	27.92400000	119.75900300
O	7.22400000	27.77000000	120.43599700
C	4.99100000	28.78800000	120.26200100
C	4.58900000	28.35500000	121.71900200
O	3.92900000	27.33099900	121.91200300
O	4.96100000	29.27800000	122.76599900
C	4.97100000	28.96400100	124.13999900
Mg	-15.55100000	25.63800000	113.53199800
C	-13.17900000	27.40300000	115.40499900

C	-18.07399900	27.34100000	115.19000200
C	-17.82799900	24.39900000	111.28800200
C	-12.97300000	24.53200000	111.47699700
N	-15.61700000	27.12800000	115.12000300
C	-14.52700000	27.71100000	115.74700200
C	-15.00800000	28.66200100	116.83300000
C	-16.46999900	28.37500000	116.94000200
C	-16.78900000	27.60800000	115.66799900
C	-16.72200000	27.51100000	118.18399800
C	-14.99200000	30.18800000	116.68900300
N	-17.59199900	25.78000100	113.32199900
C	-18.44400000	26.52300100	114.11499800
C	-19.80200000	26.33799900	113.64099900
C	-19.74300000	25.54400100	112.52600100
C	-18.34199900	25.17100000	112.34100300
C	-21.03300100	26.97600000	114.34600100
C	-21.01499900	25.28800000	111.85600300
C	-21.15600000	24.59700000	110.68000000
N	-15.41500000	24.53300100	111.76200100
C	-16.48500100	24.10000000	111.00900300
C	-16.00200100	23.35600100	109.86200000
C	-14.64400000	23.40200000	109.89800300
C	-14.27400000	24.19800000	111.06300400
C	-16.85600100	22.73000000	108.74800100
C	-13.67000000	22.67200100	108.92800100
C	-13.38300000	23.45700100	107.66600000
N	-13.52700000	25.69500000	113.55899800
C	-12.60700000	25.23500100	112.63800000
C	-11.25900000	25.65700000	113.00399800
C	-11.42000000	26.45000100	114.10500300
C	-12.82100000	26.52199900	114.38500200
C	-9.95200000	25.31699900	112.26899700
C	-10.75700000	27.27599900	115.08599900
O	-9.56800000	27.53800000	115.25299800
C	-11.85900000	27.93300100	115.98100300
C	-11.64900000	27.52800000	117.47100100
O	-11.84800000	26.38900000	117.89700300
O	-11.16400000	28.60199900	118.27400200
C	-11.08500000	28.54700100	119.65699800
Mg	-7.36600000	29.12500000	109.63200400
C	-8.49400000	30.59600100	112.63099700
C	-4.49600000	31.07099900	109.86699700
C	-6.61400000	28.43199900	106.36000100
C	-10.60900000	27.99799900	109.08100100
N	-6.53500000	30.52400000	111.13700100
C	-7.15000000	30.93700000	112.31199600
C	-6.22800000	31.86300100	113.09300200
C	-5.09600000	32.14500000	112.14199800
C	-5.33700000	31.19300100	110.97399900
C	-5.11500000	33.63100100	111.73600000
C	-5.73000000	31.38800000	114.45099600
N	-5.71300000	29.44400000	108.43299900

C	-4.65700000	30.29100000	108.71700300
C	-3.76900000	30.33200100	107.57399700
C	-4.36500000	29.62599900	106.56400300
C	-5.61700000	29.08600000	107.10199700
C	-2.41200000	31.09100000	107.60500300
C	-3.65000000	29.61400000	105.28399700
C	-4.01200000	28.87200000	104.17800100
N	-8.40000000	28.24099900	108.05300100
C	-7.89200000	28.03599900	106.78700300
C	-8.89600000	27.38800000	105.96600300
C	-10.03100000	27.31100100	106.70900000
C	-9.71700000	27.83400000	108.02300300
C	-8.76600000	26.98399900	104.48200200
C	-11.41400000	26.81200000	106.24900100
C	-12.26300000	27.95800000	105.68199900
N	-9.10500000	29.09700000	110.65899700
C	-10.34500000	28.60000000	110.31300400
C	-11.33600000	28.98800100	111.29599800
C	-10.66400000	29.71200000	112.23200200
C	-9.30900000	29.81399900	111.80699900
C	-12.82000000	28.66300000	111.24299600
C	-10.76100000	30.40399900	113.49299600
O	-11.70600000	30.57000000	114.25099900
C	-9.36700000	30.97300000	113.84100300
C	-9.47200000	32.51699800	114.06099700
O	-9.22300000	32.95500200	115.18599700
O	-9.93600000	33.31700100	112.97399900
C	-9.39000000	34.53699900	112.68199900
C	-9.24600000	23.00900100	98.13099700
C	-9.33900000	22.41200100	96.70900000
C	-9.41900000	20.89399900	96.55000300
C	-8.71900000	20.11300100	97.66100300
C	-8.70800000	20.67900100	99.04200000
C	-8.94500000	22.01400000	99.29599800
C	-8.93100000	22.54400100	100.67400400
C	-7.85700000	22.83499900	101.43499800
C	-7.87700000	23.22699900	102.84600100
C	-6.70900000	23.59000000	103.42199700
C	-6.51900000	24.02000000	104.78500400
C	-5.34500000	24.54200000	105.16999800
C	-4.93200000	25.08300000	106.47300000
C	-3.71000000	25.65600000	106.53700300
C	-3.08700000	26.32900000	107.64199800
C	-10.55700000	23.77199900	98.39700300
C	-8.11400000	24.04700100	98.01599900
C	-8.42200000	19.56100100	99.98200200
C	-9.21000000	23.25000000	103.54299900
C	-5.90900000	25.03500000	107.61000100
O	-8.91200000	20.50099900	95.28299700
C	3.82000000	34.42699800	114.84999800
C	4.18400000	35.19200100	116.13999900
C	5.29800000	34.56499900	116.98200200

C	5.29800000	33.03200100	116.95800000
C	4.59300000	32.29600100	116.07199900
C	3.69600000	32.87300100	114.98300200
C	3.86100000	32.09199900	113.67700200
C	2.87100000	31.40099900	113.05200200
C	2.87300000	30.85400000	111.68100000
C	1.77600000	30.18700000	111.26100200
C	1.56100000	29.57799900	109.97300000
C	0.41600000	28.91600000	109.71299700
C	-0.01200000	28.20800000	108.49700200
C	-1.22400000	27.61300100	108.51899700
C	-1.87200000	26.87500000	107.47300000
C	4.89000000	34.79999900	113.78600300
C	2.47700000	34.99800100	114.37400100
C	4.74300000	30.82900000	116.26300000
C	4.09800000	31.06399900	110.83999600
C	0.92800000	28.19100000	107.32000000
O	5.22500000	35.04200000	118.31900000
H	4.64972602	29.86308490	124.67055025
H	5.98772611	28.69793961	124.44289435
H	4.29149454	28.13441058	124.36128504
H	5.31126079	29.83594613	120.28529330
H	7.66326531	25.12751183	117.08290606
H	8.36042016	26.54598678	117.88866634
H	8.09086994	26.55298633	116.12789943
H	6.15326504	26.18337139	114.62867566
H	5.47915868	27.32366580	110.38091116
H	7.00111066	26.43990334	110.61046880
H	6.49388974	27.66832765	111.78959200
H	6.10951955	25.31255427	112.61814039
H	5.09468752	24.99310751	111.23204533
H	2.80873167	25.10468228	110.50382971
H	2.93741828	26.83288146	110.11504131
H	1.39359091	26.16090489	110.64524214
H	0.25736152	27.24522790	112.28441076
H	-3.43120219	28.92082619	113.55289405
H	-3.18989701	28.39729664	111.19189078
H	-1.52129364	27.66271553	111.50592264
H	-4.08745920	28.55423494	115.46310586
H	-3.39060222	30.08270654	116.04793818
H	-3.38843792	28.63287471	117.06979225
H	-1.69132382	29.03200490	118.15675280
H	-0.40900067	29.97363456	120.17901385
H	-1.07530876	27.59137606	120.66932634
H	-0.10460041	28.27627523	121.99161266
H	0.64077461	27.15993883	120.83480475
H	2.06877628	29.31710252	121.26787690
H	2.95847424	31.42670299	120.29366430
H	1.31765558	31.65058404	120.93527129
H	1.57870373	31.51315416	119.17611310
H	-11.86692715	29.17847063	120.09266714
H	-10.10628506	28.93098875	119.95575693

H	-11.20036486	27.52083755	120.02226082
H	-11.74902493	29.01847054	115.90143444
H	-9.10591628	25.51853237	112.92968439
H	-9.85208326	25.94318343	111.37395507
H	-9.93447335	24.26713514	111.96471297
H	-12.15965802	24.22184586	110.82368814
H	-12.73926758	22.45470679	109.46225355
H	-14.11476071	21.70266669	108.67940253
H	-14.31072825	23.73947051	107.15662123
H	-12.77205362	22.87873916	106.96686409
H	-12.84258199	24.37793782	107.90102669
H	-16.26490048	22.01483274	108.17036538
H	-17.22318646	23.50164205	108.06215908
H	-17.72213496	22.20043101	109.15701835
H	-18.54626536	23.97992256	110.59733915
H	-21.90125180	25.68467849	112.33784586
H	-22.14101141	24.45250298	110.24790979
H	-20.32305230	24.19585868	110.12035078
H	-21.88302774	26.29002944	114.34413446
H	-21.33829892	27.90352106	113.85055351
H	-20.79616850	27.20178595	115.38613365
H	-18.87812200	27.82691473	115.73312267
H	-17.08309414	29.27776161	117.00868229
H	-17.77471888	27.22335092	118.28205438
H	-16.43227429	28.06733695	119.08193425
H	-16.11973199	26.59797541	118.13552937
H	-14.47933769	28.40571287	117.76171166
H	-13.98797323	30.60349854	116.55215505
H	-15.42046884	30.62065889	117.59573839
H	-15.59475243	30.49933577	115.82981317
H	-10.14442923	35.11480789	112.14363064
H	-8.50566029	34.42786194	112.03985245
H	-9.10851171	35.08598431	113.58887176
H	-9.03127894	30.56076689	114.79478809
H	-13.29956305	29.17344231	110.40192018
H	-13.29936153	28.98724647	112.17074721
H	-12.97928509	27.58548548	111.12593674
H	-11.63233360	27.66624212	108.91632327
H	-11.28893039	26.02231687	105.50112256
H	-11.93285892	26.35400167	107.09808796
H	-13.26454244	27.60875965	105.41381150
H	-11.79232187	28.37735300	104.78822942
H	-12.36012664	28.76372017	106.41705832
H	-9.71839191	26.60249822	104.10841903
H	-8.00044599	26.21295810	104.34139882
H	-8.48621678	27.84823993	103.87019418
H	-6.39807059	28.25628716	105.31348266
H	-2.81085438	30.29516601	105.20281627
H	-3.44789318	28.95217790	103.25448024
H	-4.81981675	28.15133433	104.19970470
H	-2.54135625	32.14892971	107.35365881
H	-1.69936370	30.64675841	106.90768116

H	-1.97123762	31.01650424	108.60216818
H	-3.60322518	31.68915042	109.89708361
H	-4.12536807	31.91244185	112.59970929
H	-4.30350305	33.87854108	111.04416896
H	-5.02130240	34.26372968	112.62371118
H	-6.06367975	33.86394244	111.23882648
H	-6.78874332	32.79254847	113.28171077
H	-6.55084586	31.23959903	115.15879637
H	-5.18394025	30.44317478	114.35425506
H	-5.05108401	32.13870250	114.87022795
H	-9.47414240	20.90724917	94.60867603
H	-10.48331718	20.60685621	96.60776971
H	4.42224781	34.66183989	118.70533973
H	6.27719325	34.91595966	116.62992184
H	-9.25214415	18.84497274	99.97228814
H	-8.26628989	19.89141348	101.01282540
H	-7.52815830	19.01602736	99.65756895
H	5.15088026	30.32985125	115.37407489
H	3.76971311	30.34499437	116.44906662
H	5.39123704	30.60032358	117.11101662
H	-9.13803190	19.09976648	97.67862888
H	5.91197429	32.56071903	117.72095492
H	-7.15745573	23.55043166	97.81984855
H	-8.00984887	24.63687238	98.93451760
H	-8.32405936	24.73459851	97.18899456
H	-10.53913016	24.27945591	99.36750352
H	-11.41530225	23.09068011	98.38547199
H	-10.71042216	24.53221108	97.62431828
H	4.61696043	34.42162030	112.79609774
H	5.87329253	34.39111654	114.05075055
H	4.98006465	35.88853414	113.71682790
H	1.69600058	34.83839621	115.12748800
H	2.15336463	34.51955971	113.44298950
H	2.55876029	36.07551967	114.19256490
H	4.41841796	36.23246307	115.89822008
H	3.29551935	35.21384194	116.78857089
H	-10.17135516	22.87922517	96.16901492
H	-8.42819726	22.68643063	96.16289565
H	2.66593848	32.66207116	115.32070897
H	4.83512298	32.17780000	113.19433591
H	1.91419137	31.31910164	113.57237142
H	3.99695154	30.65304333	109.83611669
H	4.96876279	30.59171042	111.31265721
H	4.32336654	32.13308397	110.75032522
H	0.95078237	30.08110950	111.96706152
H	2.34183277	29.63700511	109.21676629
H	-0.32813194	28.92354067	110.50886499
H	0.54168742	27.61286816	106.48029918
H	1.89400570	27.76435094	107.61027056
H	1.12065146	29.21234828	106.97246228
H	-1.81233986	27.71767758	109.42715492
H	-1.38100728	26.76905240	106.50811951

H	-3.60341301	26.43193754	108.59407140
H	-3.10873634	25.63131677	105.62781622
H	-5.50170057	25.46539080	108.52647645
H	-6.20379988	24.00108904	107.82130756
H	-6.82174795	25.59012104	107.35402970
H	-4.56317757	24.59048594	104.40877664
H	-7.34527927	23.95708717	105.49077714
H	-5.81207623	23.57799209	102.80305236
H	-9.88049659	23.96688368	103.05077988
H	-9.13204920	23.53386200	104.59274373
H	-9.69157177	22.26739124	103.48587297
H	-6.86810228	22.71097097	100.98968549
H	-9.91856350	22.70253558	101.11502071
H	-7.67116114	19.97613086	97.34400798

Nuclear coordinates of the carotenoid in system M':

C	-9.9741533045	22.1948953205	98.2563441250
C	-9.6020797256	21.7458739692	96.8321993647
C	-9.1408923775	20.2991620288	96.7702604526
C	-7.8956669479	20.1317798990	97.6196355492
C	-7.9859289675	20.7915447960	98.9787667681
C	-8.8981645423	21.7476990808	99.2639993956
C	-8.9714311009	22.4277676315	100.5682099260
C	-7.9235010100	22.9735400710	101.2372332400
C	-7.9989686806	23.6664296874	102.4964362925
C	-6.8198937968	24.1872676114	103.0275583801
C	-6.6546484471	24.8900930691	104.2227984817
C	-5.3869814432	25.3576073694	104.6491060030
C	-5.0857396361	26.0448166581	105.8026379581
C	-3.7026477337	26.4251384068	106.0304856639
C	-3.2284686707	27.0998180217	107.1023766837
C	-11.3411635752	21.6054415505	98.6577222336
C	-10.0884904279	23.7295742347	98.2437515368
C	-6.9583445809	20.2740632250	99.9535544525
C	-9.3352433381	23.7994924676	103.1737397894
C	-6.1071977653	26.4210251838	106.8405273862
O	-8.8062743977	19.9008005750	95.4467777956
C	4.0230432861	34.2678717327	115.0417203030
C	4.1393764376	34.8613788258	116.4550036760
C	5.3377270679	34.3202325839	117.2285646315
C	5.4073132618	32.8215062085	117.1202608676
C	4.7356905700	32.0933298420	116.2227259388
C	3.8176362345	32.7262250369	115.1788361075
C	3.9352333799	32.0175809716	113.8548469518
C	2.8908538437	31.4813669310	113.1898097291
C	2.9525553126	30.8062192334	111.9116246689
C	1.7730416389	30.3068900567	111.3780044752
C	1.5992838932	29.6225419623	110.1661450794
C	0.3335325574	29.1684568443	109.7377344421
C	0.0272133282	28.4920181781	108.5738966913

C	-1.3539169551	28.1174785245	108.3453908758
C	-1.8300277720	27.4466230177	107.2701926924
C	5.2825748694	34.5979429149	114.2238261533
C	2.8061210702	34.8859070789	114.3453749155
C	4.8028900804	30.5893393679	116.2237487874
C	4.2880327696	30.6809577873	111.2322167326
C	1.0486109132	28.1229313738	107.5334085436
O	5.3117183634	34.7337347240	118.5929879481
H	-9.6077889512	19.9840646989	94.9128760641
H	-9.9313294085	19.6418962266	97.1632101817
H	4.5294475196	34.3250239256	118.9901886140
H	6.2622962748	34.7635877407	116.8382003774
H	-6.8960359023	19.1808636932	99.8866087080
H	-7.1774073733	20.5417544209	100.9890738376
H	-5.9578370093	20.6586369280	99.7124221666
H	5.2715666344	30.2045359860	115.3098955018
H	3.7942707545	30.1572408243	116.2611419920
H	5.3700650320	30.2156891503	117.0819301222
H	-7.6700635225	19.0652926798	97.7402750708
H	6.0423175219	32.3261238897	117.8547469547
H	-9.1174696524	24.1953603800	98.0396397469
H	-10.4557427433	24.1215962076	99.1982400448
H	-10.7890052067	24.0466722024	97.4613967778
H	-11.6470260947	21.9432177960	99.6541700163
H	-11.3250076097	20.5107015581	98.6701232930
H	-12.1152078619	21.9287398515	97.9507059458
H	5.1421376842	34.3499621674	113.1660377017
H	6.1629825316	34.0514446095	114.5799387779
H	5.5024620643	35.6704884126	114.2854353246
H	1.8907893396	34.7234517551	114.9279261037
H	2.6551830418	34.4525479763	113.3503374073
H	2.9410393307	35.9675439268	114.2246104081
H	4.1986705372	35.9552894078	116.4020282470
H	3.2276173706	34.6134599117	117.0189748770
H	-10.4662071814	21.8983392097	96.1705297694
H	-8.7867102113	22.3739983266	96.4483391250
H	2.7872312306	32.5730683900	115.5380098824
H	4.9366975893	31.9522278443	113.4322822765
H	1.9018234568	31.5564229655	113.6451658598
H	4.2273399897	30.1807149787	110.2641292280
H	4.9904085448	30.1148249682	111.8571359790
H	4.7334792623	31.6702254833	111.0684857429
H	0.8711369905	30.4658128433	111.9716581833
H	2.4648188293	29.4342030376	109.5378535475
H	-0.5000620953	29.3790934086	110.4099922584
H	1.0902398462	27.0348582676	107.3982106503
H	2.0535358695	28.4652699655	107.7860416717
H	0.7844728692	28.5557434838	106.5605244377
H	-2.0638361684	28.4085467604	109.1209933714
H	-1.1528746076	27.1370337200	106.4749801877
H	-3.9060343428	27.4110188572	107.8966541713
H	-2.9923954305	26.1313146847	105.2562532997

H	-6.0616181676	25.4454160615	107.4189521977
H	-7.1081608163	26.3058434417	106.5024258208
H	-5.8652870480	27.0575130656	107.6677812880
H	-4.5529243991	25.1420199051	103.9790720676
H	-7.5214684735	25.0853773882	104.8472595939
H	-5.9161632332	24.0223498507	102.4383634266
H	-10.0355205327	24.3644421459	102.5451424884
H	-9.2731288551	24.3069321359	104.1379636366
H	-9.7842087373	22.8136011871	103.3455770404
H	-6.9333882944	22.9071010696	100.7873391574
H	-9.9709630285	22.5587290454	100.9812297619
H	-7.0447384691	20.5606205439	97.0684656115

Nuclear coordinates of the carotenoid in system M″:

C	-13.3106734418	23.5212890715	103.0588185855
C	-13.8689837861	23.7379697063	101.6418270543
C	-13.6738851378	22.5327098474	100.7372272631
C	-12.1920639986	22.2439934389	100.5932850901
C	-11.4152236758	22.3086459114	101.8903915418
C	-11.8851957600	22.9369628391	102.9945450323
C	-11.1194195266	23.0767761883	104.2368201875
C	-9.7875054592	23.3465480544	104.3562576562
C	-9.0843570739	23.5597804603	105.5829476624
C	-7.7393689514	23.9497891722	105.5201900019
C	-6.9889970147	24.4554781418	106.5693535178
C	-5.6584855753	24.9392878990	106.4351445775
C	-4.9487890918	25.6160404492	107.3909665602
C	-3.5976532447	26.0788591150	107.0995327281
C	-2.9173126239	26.9321652219	107.8924271569
C	-14.2218582085	22.5595924542	103.8494311011
C	-13.3198810190	24.8877960475	103.7683830327
C	-10.0760477852	21.6184642149	101.8114432631
C	-9.8125667086	23.4421387151	106.8945011150
C	-5.5033871868	25.9269122730	108.7554711596
O	-14.1872199199	22.7558587478	99.4308193963
C	3.3380472436	33.3303168291	116.2095909963
C	3.3973519765	33.7972172008	117.6733588131
C	4.7980827061	33.7358598983	118.2726090946
C	5.4708096851	32.4336968943	117.9403214364
C	5.0646774101	31.5916316811	116.9848549344
C	3.8114766183	31.8420082907	116.1504212683
C	3.9980900600	31.3614999962	114.7321977473
C	3.0423816018	30.7697024744	113.9894868768
C	3.1888030893	30.3456502933	112.6100901570
C	2.0451151604	30.0265852285	111.9047041713
C	1.9308619869	29.5632102732	110.5822687066
C	0.6737872673	29.2254956482	110.0501183920
C	0.3707327568	28.5834351088	108.8619125086
C	-1.0047664183	28.1952842989	108.6733732028
C	-1.5404801810	27.3599471164	107.7493548725

C	4.2270459316	34.2226369522	115.3286036412
C	1.8876086615	33.4381983609	115.7259724227
C	5.8304289297	30.3330366005	116.6782290513
C	4.5700555448	30.2819467462	112.0208786214
C	1.3968407220	28.1686191143	107.8460890619
O	4.7802362166	33.9771999630	119.6771267914
H	-15.1392605186	22.8927388781	99.5129447740
H	-14.1668385260	21.6541088818	101.1795951517
H	4.2950406489	33.2471026927	120.0831667707
H	5.4031925666	34.5619022173	117.8780059322
H	-10.1599573780	20.7060271576	101.2101163568
H	-9.6848018451	21.3463683572	102.7940485529
H	-9.3265675711	22.2510093666	101.3166420946
H	6.4150608296	30.4409760479	115.7564760117
H	5.1522505022	29.4895842055	116.5174330217
H	6.5240116822	30.0788866711	117.4843725562
H	-12.0520343263	21.2637031543	100.1224746862
H	6.3677413037	32.2064440931	118.5162598112
H	-12.5867045393	25.5707660770	103.3243274277
H	-13.0962851206	24.7975109581	104.8360518601
H	-14.3113852586	25.3474237408	103.6788087317
H	-13.8503324354	22.4087652585	104.8683857465
H	-14.2855551164	21.5761462965	103.3742136295
H	-15.2349621687	22.9728901000	103.9265060627
H	4.0783553628	33.9938585021	114.2681045075
H	5.2907999991	34.0891373804	115.5535005514
H	3.9758737976	35.2784313811	115.4827445351
H	1.2191373637	32.8232022154	116.3415291850
H	1.7889626487	33.1109540717	114.6861576030
H	1.5430430829	34.4770324512	115.7869846411
H	3.0066108939	34.8183346825	117.7593475483
H	2.7408358123	33.1534275743	118.2741448422
H	-14.9360040303	23.9919398470	101.7117883641
H	-13.3646490735	24.5943195136	101.1741305822
H	3.0089497371	31.2338661417	116.6018644683
H	4.9671845981	31.5662424651	114.2803912977
H	2.0608162237	30.6061638329	114.4391155594
H	4.5852021964	29.8057751023	111.0389855969
H	5.2359838759	29.7122623216	112.6793571738
H	5.0018143756	31.2850874978	111.9110625308
H	1.1059204925	30.1156198633	112.4517881004
H	2.8260275971	29.4085190770	109.9862603281
H	-0.1739569952	29.4407304179	110.7026993868
H	1.5189317472	27.0777110617	107.8419511176
H	2.3759880688	28.6147263645	108.0328433871
H	1.0816948074	28.4597962902	106.8373742312
H	-1.6930936170	28.5789641479	109.4239582242
H	-0.9403717770	26.9382635329	106.9447182849
H	-3.4216669261	27.3370542217	108.7679199946
H	-3.1299484533	25.7032334791	106.1893661067
H	-4.8451659821	25.5352136155	109.5398262188
H	-6.5025234320	25.5221922245	108.9157240135

H	-5.5596184867	27.0126932842	108.8914232126
H	-5.1786933644	24.7872129279	105.4670462647
H	-7.4709345855	24.5565788982	107.5355055193
H	-7.2679963525	23.9253185111	104.5361908374
H	-10.4679388436	24.3048822737	107.0663049937
H	-9.1273859970	23.3696623744	107.7411629837
H	-10.4411617970	22.5457293628	106.9110146502
H	-9.2031694326	23.4791806971	103.4478040794
H	-11.7047062912	23.0404970036	105.1527544497
H	-11.7710805690	22.9781867402	99.8891680893

1. J. Ho, E. Kish, D. D. Méndez-Hernández, K. WongCarter, S. Pillai, G. Kodis, J. Niklas, O. G. Poluektov, D. Gust, T. A. Moore, A. L. Moore, V. S. Batista and B. Robert, Triplet-triplet energy transfer in artificial and natural photosynthetic antennas, *Proc. Natl. Acad. Sci. U.S.A.*, 2017, **114**, E5513-E5521.
2. J. D. Chai and M. Head-Gordon, Long-range corrected hybrid density functionals with damped atom-atom dispersion corrections, *Phys. Chem. Chem. Phys.*, 2008, **10**, 6615-6620.
3. M. J. Frisch, G. W. Trucks, H. B. Schlegel, G. E. Scuseria, M. A. Robb, J. R. Cheeseman, G. Scalmani, V. Barone, G. A. Petersson, H. Nakatsuji, X. Li, M. Caricato, A. V. Marenich, J. Bloino, B. G. Janesko, R. Gomperts, B. Mennucci, H. P. Hratchian, J. V. Ortiz, A. F. Izmaylov, J. L. Sonnenberg, D. Williams-Young, F. Ding, F. Lipparini, F. Egidi, J. Goings, B. Peng, A. Petrone, T. Henderson, D. Ranasinghe, V. G. Zakrzewski, J. Gao, N. Rega, G. Zheng, W. Liang, M. Hada, M. Ehara, K. Toyota, R. Fukuda, J. Hasegawa, M. Ishida, T. Nakajima, Y. Honda, O. Kitao, H. Nakai, T. Vreven, K. Throssell, J. A. Montgomery, J. E. Peralta, Jr. , F. Ogliaro, M. J. Bearpark, J. J. Heyd, E. N. Brothers, K. N. Kudin, V. N. Staroverov, T. A. Keith, R. Kobayashi, J. Normand, K. Raghavachari, A. P. Rendell, J. C. Burant, S. S. Iyengar, J. Tomasi, M. Cossi, J. M. Millam, M. Klene, C. Adamo, R. Cammi, J. W. Ochterski, R. L. Martin, K. Morokuma, O. Farkas, J. B. Foresman and D. J. Fox, Gaussian 16, Revision B.01; Gaussian, Inc., Wallingford CT, 2016.
4. T. Yanai, D. P. Tew and N. C. Handy, A new hybrid exchange-correlation functional using the Coulomb-attenuating method (CAM-B3LYP), *Chem. Phys. Lett.*, 2004, **393**, 51-57.
5. L. Li, C. Li, Z. Zhang and E. Alexov, On the 'Dielectric "Constant" of Proteins: Smooth Dielectric Function for Macromolecular Modeling and Its Implementation in DelPhi, *J. Chem. Theory Comput.*, 2013, **9**, 2126-2136.
6. V. Sláma, L. Cupellini and B. Mennucci, Exciton properties and optical spectra of light harvesting complex II from a fully atomistic description, *Phys. Chem. Chem. Phys.*, 2020, **22**, 16783-16795.
7. C. Curutchet, A. Muñoz-Losa, S. Monti, J. Kongsted, G. D. Scholes and B. Mennucci, Electronic Energy Transfer in Condensed Phase Studied by a Polarizable QM/MM Model, *J. Chem. Theory Comput.*, 2009, **5**, 1838–1848.
8. A. Sirohiwal, R. Berraud-Pache, F. Neese, R. Izsák and D. A. Pantazis, Accurate Computation of the Absorption Spectrum of Chlorophyll *a* with Pair Natural Orbital Coupled Cluster Methods, *J. Phys. Chem. B*, 2020, **124**, 8761−8771.
9. Z. F. Liu, H. C. Yan, K. B. Wang, T. Y. Kuang, J. P. Zhang, L. L. Gui, X. M. An and W. R. Chang, Crystal structure of spinach major light-harvesting complex at 2.72 Å resolution, *Nature*, 2004, **428**, 287-292.